INTERNATIONAL JOURNAL OF HYDROGEN ENERGY 49 (2024) 625–645

Available online at www.sciencedirect.com

ScienceDirect

journal homepage: www.elsevier.com/locate/he

Review Article

Electrical circuit modeling of proton exchange membrane electrolyzer: The state-of-the-art, current challenges, and recommendations

Mohamed Khalid Ratib[*], *Kashem M. Muttaqi*, *Md Rabiul Islam*, *Danny Sutanto*, *Ashish P. Agalgaonkar*

Australian Power and Energy Research Institute (APERI), School of Electrical, Computer, and Telecommunications Engineering, Faculty of Engineering and Information Sciences, University of Wollongong, New South Wales, 2522, Australia

HIGHLIGHTS

- A comprehensive review of the electrical circuit models of the PEM electrolyzer is presented.
- The models are classified in terms of voltage components, model behavior, and scale.
- Simulations of the models are implemented to show their similarities and deviations.
- Applications, benefits, and drawbacks of electrical circuit modeling are discussed.
- Overarching technical recommendations are drawn for further research on electrical circuit modeling.

ARTICLE INFO

Article history:
Received 9 June 2023
Received in revised form
6 August 2023
Accepted 28 August 2023
Available online 27 September 2023

Keywords:
PEM electrolyzer
Electrical circuit modeling
Renewable energy sources
PEM electrolyzer modeling
Generation of hydrogen from RESs

ABSTRACT

The integration of water electrolysis with renewable energy sources (RESs) constitutes a milestone in the transition to neutral and sustainable energy systems. The attractive features of the Proton Exchange Membrane (PEM) electrolyzer such as high purity of hydrogen, operation with high pressure, and high current densities have made it a critical technology to produce green hydrogen from RESs. Accurate models are required for proper design, analysis, and control of the electrolyzer when connected to the grid or renewable energy systems. Amongst the various types of models proposed for modeling the PEM electrolyzer, electrical circuit models are the easiest, most appealing, and straightforward to use for the investigation of electrolyzer operation and control. This paper presents an exhaustive review of the electrical circuit modeling reported in the literature on PEM electrolyzers. The reviewed models are classified analogously to the classifications of physical modeling in terms of voltage components (reversible, ohmic, activation, and concentration voltage drop), model behavior (static/dynamic), and modeling scale (cell/stack). Furthermore, MATLAB simulations of the reviewed models are implemented and the results are compared to pinpoint their similarities and deviations. Moreover, the applications, challenges, benefits, and drawbacks of the electrolyzer's electrical equivalent circuit modeling are discussed and overarching recommendations are set out for further research on the PEM electrolyzer modeling. The paper can be used as a comprehensive

* *Corresponding author.*
E-mail addresses: mkrt166@uowmail.edu.au (M. Khalid Ratib), kashem@uow.edu.au (K. M. Muttaqi), mrislam@uow.edu.au (M.R. Islam), soetanto@uow.edu.au (D. Sutanto), ashish@uow.edu.au (A.P. Agalgaonkar).
https://doi.org/10.1016/j.ijhydene.2023.08.319

reference for choosing the appropriate electrical model of the electrolyzer for beginners as well as for research and industry experts who rely on PEM electrolyzer models in their work.

List of symbols

$\Delta G(T)$	Change in Gibbs free energy of reaction
ΔS	Change in the entropy of the reaction species
ΔH	Change in the enthalpy of the reaction species
P_{cell}	Electric power consumption of the electrolysis cell (i.e., cell power) in Watt
E_{cell}	Cell terminal voltage in Volt
I_{cell}	Cell current in Ampere
$E_{rev}(T,P)$	The reversible voltage at arbitrary values of temperature and pressure
$E_{rev}(STP)$	The reversible voltage at standard values of temperature and pressure
E_{ohm}	Ohmic overvoltage (i.e., overpotential)
E_{act}	Activation overvoltage (i.e., overpotential)
$E_{act}(0)$	Initial value of the activation overvoltage
$E_{conc/diff}$	Concentration/Diffusion overvoltage (i.e., overpotential)
V_{DC}	DC voltage source
V_{int}	The constant value of the reversible voltage in electric circuit representations
V_{th}	Thermoneutral voltage
P_{H_2}	The pressure of hydrogen at the cathode compartment in *KPa*
P_{O_2}	The pressure of oxygen at the anode compartment in *KPa*
a_{H_2O}	Water activity coefficient
P_{output}	Cell's output pressure
P_{Input}	Cell's input pressure
n_{H_2}	Hydrogen stoichiometric number ($n_{H_2} = 2$)
n_{O_2}	Oxygen stoichiometric number ($n_{O_2} = 4$)
$\eta_{act,k}$	Activation overpotential of compartment k
$\eta_{conc,k}$	Concentration overpotential of compartment k
τ_k	The time constant of compartment k
C_k	The capacitance value of compartment k
τ_{tot}	Total time constant of the anode and cathode compartments combined
C_{dl}	Double-layer capacitance
R_{ohm}	Resistance related to the ohmic overvoltage
R_{act}	Resistance related to the activation overvoltage
R_{mass}	Resistance due to the mass transfer effect and related to the concentration overvoltage
Z_{wbg}	Warburg impedance
i_c	Capacitor current
i_R	Resistor current
t_c	Time at which current I_1 changes to current I_2
F	Faraday constant, $F = 96.485\ \frac{KJ}{mol}$
R	Ideal gas constant $R = 8.314\ \frac{J}{K \cdot mol}$ *or* $J\ .K^{-1}\ .\ mol^{-1}$

Contents

1. Introduction

The continuously growing world population, industrial, and technological advancements are the main reasons behind increased amounts of air pollutants, global temperature rise, sea water level rise, climate change, and other major environmental problems [1]. Electrical power generation, industrial enterprises, and transportation are estimated to account

for 40%, 23%, and 23% of the global carbon emissions respectively, while the remaining 14% are coming from different sources [2,3]. Many countries around the world have set out serious and multidisciplinary initiatives for reducing local and global carbon capture and mitigating the effects of climate change [4,5]. In this regard, the Australian Government has created Australia's Long-Term Emissions Reduction Plan which takes responsible and practical actions on the whole of the economy to help Australia set out its pathway to deliver net zero emissions by 2050 [6].

Fossil fuels have almost exclusively powered global economic growth since the start of the industrial revolution at the beginning of the 19th century [7]. As countries act on climate change, considerable efforts have been carried out to reduce the share of the three major sources of carbon emissions stated above. As a result, in the energy sector, several scenarios have been considered for generating electricity from renewable energy sources (RESs), especially wind, solar, wave and tidal, and hydropower [8,9]. In addition to decarbonizing the energy sector using RESs, the greenhouse emissions from the industrial and transportation sectors are to be reduced by incorporating clean fuels for shrinking down the carbon emissions of heavy industries and long-distance transportation systems, which are difficult to be electrified [1]. A great deal of interest has been raised in the industry and academia fraternity for hydrogen to be considered as the fuel of future, because of its versatility and multidisciplinary applications. It is expected to play a key role in the transition to a clean and sustainable future [10,11]. Hydrogen can be used as a clean, sustainable energy carrier and long-term energy storage medium as well as carbon-free fuel for transportation, aviation, heavy manufacturing processes, and chemical industry applications [12].

Solar and wind power generation completely depends on the weather. When there is a high penetration of these renewable resources, the intermittent nature and the highly irregular spatial distribution of these resources can lead to prodigious time-varying discrepancies between the energy supply and demand [13,14]. Therefore, energy storage technologies are usually used to store the excess generation of renewable energy (RE) in times of abundance of wind and/or solar irradiation and to use this stored energy to compensate for the shortage in generation when there is a lack of wind or sunlight [15]. The integration of water electrolysis to generate hydrogen using electricity from the excess energy of RESs can help overcome the sporadic nature of RESs while also reducing the costs of green hydrogen production [1,16]. The generated hydrogen is usually stored in high-pressure tanks, and when required, the hydrogen can be sent to hydrogen retailers or used to generate electricity back through fuel cells. The system dedicated to optimizing and organizing this process is often referred to as the hydrogen energy storage system.

Water electrolysis uses water electrolyzers to convert electrical energy into chemical energy in the form of hydrogen. Water electrolyzers can be divided into alkaline water electrolyzer (AWE), proton exchange membrane water electrolyzer (PEMWE), anion exchange membrane water electrolyzer (AEMWE), solid oxide electrolysis cell (SOEC), and proton conducting ceramic electrolyzer (PCCEL). Amongst these, AWE is the cheapest and most mature technology for the generation of hydrogen using electricity. However, the slow response and the incompatibility with fluctuating power sources such as RESs result in a substantial deterioration in performance when the power supply changes [17]. On the contrary, PEMWE has a faster response, operates with higher current densities, produces high-pressure hydrogen output, and shows less performance degradation with on/off switching and repeated changes in the power supply voltage which makes it a perfect choice to operate with RESs [1,4,6].

Proper operation and control of the RE-based electrolyzers and hydrogen storage systems require accurate and comprehensive models of the system components and especially the electrolyzer [18,19]. Different models have been developed in the literature for emulating the static and dynamic characteristics of the PEM electrolyzer. Some models are developed based on the laws of thermodynamics to describe the physical, thermal, and electrochemical phenomena that happen in the electrolyzer plates and compartments [7,20–32]. Some other models are developed based on electrical laws such as Kirchhoff's current and voltage laws and the capacitance effect occurs in the electrolyzer due to the accumulation of charge on both sides of the membrane [12,13,33–41]. A third group of models is developed to approximate the performance of the electrolyzer using empirical correlations and fitting parameters based on experimental results of the electrolyzer's characteristic curve [42–45].

The area of PEMWE modeling is quite new and a limited number of reviews have been carried out on it. In addition to providing a better understanding of the state-of-the-art procedures in electrolyzer modeling, review papers give a big picture of the methods, theories, and guidelines used for model development [46]. A summary of the review papers conducted on PEM electrolyzer modeling is presented in Table 1 along with their main achievements and limitations.

Physical modeling reviews are extensively reported in the literature, however, review papers that consider the electrical modeling of the electrolyzer are very rarely reported, and if found, are not inclusive. The most extensive review article reported on electrical modeling covered only three model circuits with different assumptions and operating conditions based on the implementations of their original papers. The electrical models, therefore, have never been organized nor referred to a general base of assumptions regarding their development. Therefore, this paper aims to present a comprehensive modeling overview to gather, reorganize, and classify the electrical circuit models of the PEM electrolyzer. Furthermore, this paper presents the electrolyzer's basic principles of operation in addition to an all-inclusive investigation of the models, assumptions, and equations available in the literature on PEM electrolyzer's electrical modeling.

Thus, the novelty and contributions of this paper can be stated as follows:

- This paper is dedicated to studying, analyzing, and organizing the electrical circuit models of the PEM electrolyzer, while most review papers reported in the literature consider only physical models of the electrolyzer.
- This paper presents a review of all types of electrical models reported in the literature for modeling the PEM

Table 1 – Summary of review papers published on PEM electrolyzer modeling.

Year	Modeling approach	Contributions	Limitations	Refs.
2023	Physical, electrical	• Included a combination of electrical and physical models. • Provided a brief review of the DC/DC converters used for electrolyzer operation.	• The review only covers some of the models available either physical or electrical. • Traditional and incomprehensive classification of the models.	[40]
2022	Physical	• Developed an open-source MATLAB toolbox for modeling and parameterization of PEM and alkaline electrolyzers. • Classified the models into empirical, semi-empirical, and analytical models.	• The models consider only the static behavior of the electrolyzer. • Thermal and mass transfer sub-models are not included.	[47]
2022	Electrical	• Developed a simulation platform to analyze the behavior of the electrolyzer based on electrical models.	• The paper reviewed only three electrical models for the PEM electrolyzer. • No mention of the classification of these models.	[48]
2020	Physical	• Divided the models into empirical, semi-empirical, and analytical models. • Gave special attention to dynamic modeling, thermal, and two-phase flow effects on models' development.	• Did not cover all equations proposed in the literature for electrolyzer overpotentials. • Nor it mentioned any information about the electrical modeling of the electrolyzer.	[46]
2020	Electrical	• Investigated the electrical dynamic modeling of the electrolyzer. • Compared between the static and dynamic electrical models of the electrolyzer.	• It covered only one model of the electrical models available. • Considered only current step response for its investigations.	[49]
2017	Physical	• Classified models based on their physical domain, modeling scale, type of behavior (static or dynamic), and used modeling approach (empirical or analytical).	• Did not consider the electrical modeling of the system.	[50]
2016	Physical	• Divided the models into analytical, semi-empirical, and mechanistic models. • Provided a detailed explanation of the mass transfer phenomena that happens in the electrolyzer.	• Did not consider the thermal modeling of the system. • Its model classifications were broad and not comprehensive. • No mention of electrical modeling.	[51]

electrolyzer, while most review papers only present one or two of these electrical models.
- The assumptions that are used to simplify the modeling procedure of the PEM electrolyzer for certain applications and operating conditions are compiled, organized, and generalized, in this paper, and the effects of each assumption on the model development are clearly explained.
- In this paper, the electrical models are classified analogously to the physical models in an attempt to show the similarities and differences between these models to highlight the shortcoming of existing electrical models in describing the behavior of the PEM electrolyzer.
- The research highlights the important role electrical models play in studying the series-parallel operation and in investigating different control strategies that could be developed to improve the performance of PEM electrolyzers when integrated with RESs.

The rest of this paper is organized as follows: Section 2 is devoted to introducing a coherent explanation of the basic construction and principles of operation of the PEM electrolyzer. Section 3 inaugurates the review of various PEM electrolyzer models by first describing the modeling concepts and then instigating a comprehensive review of the electrical circuit models. Section 4 presents a brief discussion of the main findings and aspects of the studied models. Section 5 presents the challenges of applying the electrolyzer models and control strategies to large-scale systems. Section 6 briefly presents the authors' suggestions and recommendations for future research work on the electrolyzer electrical modeling area. Finally, Section 7 concludes the work presented in this study.

2. Basic construction and principles of operation

2.1. *Basic construction of the PEM electrolyser*

A PEM electrolyzer is a static electrochemical device that converts electrical energy into chemical energy mainly through the dissociation of water (the input) into oxygen and hydrogen (the output) with the help of electric direct current (DC) [52]. The PEM electrolyzer's stack consists of several electrolysis cells connected in series. Each electrolysis cell consists of three main parts namely the anode compartment, the cathode compartment, and the membrane electrode assembly (MEA) [53]. As depicted in Fig. 1, the anode compartment (which is the same as the cathode but with different types of materials) consists of three layers: the current collector layer, the gas diffusion layer, and the bipolar or flow field plates. The MEA is made of a solid polymer electrolyte (SPE) membrane (which is a thin proton conducting polymeric film) in addition to one catalyst layer on each side of the membrane. The central part of the SPE is a fiber plate used as mechanical reinforcement for the thin membrane film [54].

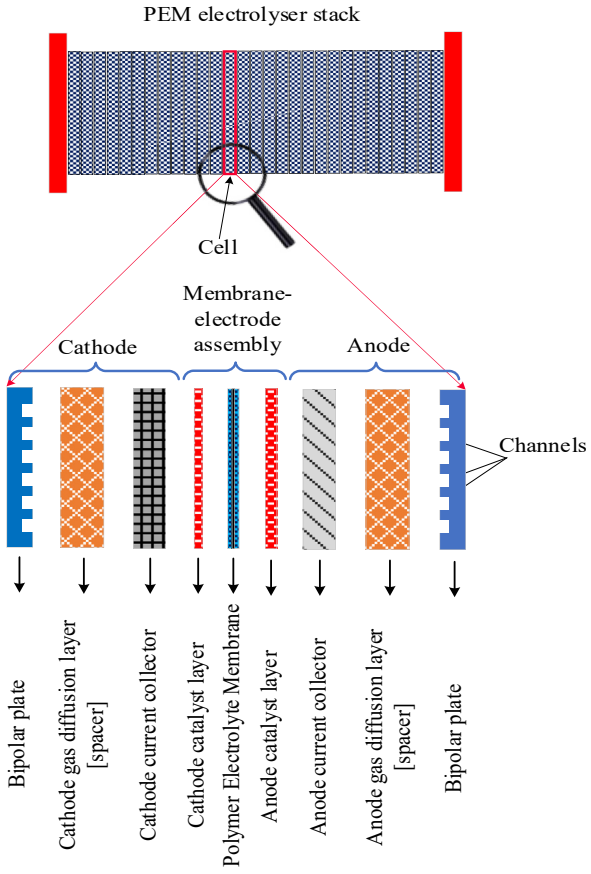

Fig. 1 – Basic construction of PEM electrolyzer cell [54].

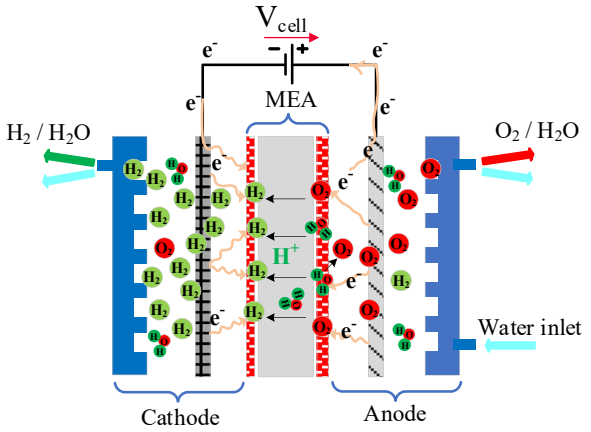

Fig. 2 – Water dissociation electrochemical reaction inside the PEM electrolysis cell [31].

The majority of models presented in the literature and all models reviewed in this paper are developed to emulate the performance of one cell only. It is worth noting that all authors assumed that the stack behavior can be estimated through the multiplication of the cell parameters (such as voltage, current, and resistance) by the number of series and parallel cells in the stack, which is not a very accurate estimation though. The word electrolyzer, if stated by itself throughout this paper, will refer always to the PEM electrolyzer.

2.2. *Principle of operation*

Water can be fed to the electrolysis cell through both the anode and cathode sides, however, in this paper (and typically for the PEM electrolysis cells), it is assumed that the water is only fed to the anode side of the cell. When the water is fed into the anode inlet, it starts to permeate through the spacer or gas diffusion layer and then from it through the porous current collector plate until it reaches the anode catalyst layer, that layer which is in direct contact with the PEM membrane [31]. Fig. 2 shows the chemical process that happens inside the electrolysis cell.

Once the electrical voltage is applied through the cell terminals and it is large enough, electrons on the surface of the current collector gain enough energy to jump out of the electrode surface and travel through the catalyst layer where they collide with the water molecules splitting them into oxygen gas, positively charged hydrogen protons, and more free electrons [33]. This process can be expressed by the anode half-cell oxidation reaction in (1) [33,55]:

$$\textit{Anode oxidation reaction}: (H_2O)_l \rightarrow \frac{1}{2}(O_2)_g + 2\,H^+ + 2\,e^- \quad (1)$$

When this reaction occurs and persists, the generated oxygen gas starts to permeate through the penetrable current collector electrode and then spread across the anode gas diffusion layer to channels of the flow field plate to find its way to the oxygen gas outlet. The generated electrons also find their way across the external circuit to the negative terminal of the power supply [56,57].

Similarly, the positively charged hydrogen protons are attracted by the existing electric field finding their way through the PEM membrane (which is a good proton conducting medium) to the cathode side of the cell. Once they are in the cathode catalyst layer, they recombine with free electrons from the cathode current collector electrode to form pure hydrogen gas [58]. The generated hydrogen gas then moves from the catalyst and porous current collector layers and across the gas diffusion layer to the bipolar (or flow field) plate which has built-in channels embedded into it to direct this gas (after acquiring a specific level of pressure) to the hydrogen outlet port of the cell. The chemical process that occurs in the cathode plates can be explained using the half-cell reduction reaction in (2) [33,59]:

$$\textit{Cathode reduction reaction}: 2\,H^+ + 2\,e^- \rightarrow (H_2)_g \quad (2)$$

Accordingly, the overall electrochemical Redox (Reduction and Oxidation) reaction that occurs in the electrolysis cell (excluding the required energy for it to happen) can be expressed as follows:

$$\textit{Overall reaction}: (H_2O)_l \rightarrow (H_2)_g + \frac{1}{2}(O_2)_g \quad (3)$$

where, g and l refer to gas and liquid, respectively.

The water electrolysis reaction is not spontaneous, for this reaction to happen an external source of energy should supply

a specific amount of it, without which there will be no splitting of the water molecules. This amount of energy or work to be done consists of a thermal part and an electrical part [46]. Under standard temperature and pressure conditions (STP), the amount of thermal energy needed by the reaction should be 48.6 kJ/mol while its electrical counterpart is supposed to be 237.2 kJ/mol, as expressed in (4) which will result in a terminal voltage equal to the reversible voltage [59,60].

$$(H_2O)_l + 237.2\ kJ/mole_{(Gibbs,electric)} + 48.6\ kJ/mole_{(Heat)} \rightarrow (H_2)_g + \frac{1}{2}(O_2)_g \quad (4)$$

However, when there is no supply of thermal energy, all the energy required by the electrolysis reaction (285.83 kJ/mol) would be supplied by the electrical source requiring it to increase the cell terminal voltage to a higher value, referred to as the thermoneutral voltage [56].

$$E_{rev}(STP) = \frac{\Delta G(T)}{n_{H_2} \cdot F}\bigg|_{T=STP} = \frac{237.2 * 10^3}{2*96485.33} = 1.22911\ \ Volts \quad (5)$$

$$V_{th} = \frac{\Delta H}{n_{H_2} \cdot F} = \frac{285.83 * 10^3}{2*96485.33} = 1.481\ Volts \quad (6)$$

3. PEM electrolyzer modeling

3.1. Modeling concepts

The electrical voltage consumed by an electrolyzer is the sum of the different voltage drops due to the reversible and irreversible processes that happen when the electrolyzer is turned on [61]. Ideally, water electrolysis is a reversible process which means that with some amount of energy the water molecules can be split into oxygen and hydrogen (electrolyzer operation) and the opposite is true when recombining oxygen and hydrogen, water and energy will be produced (fuel cell operation). Accordingly, the amount of voltage consumed by the water-splitting reaction is usually called the reversible voltage [56,62]. The amount of voltage consumed due to the irreversible processes such as: i) initiating the electrochemical reaction by moving electrons from and to the current collectors, ii) overcoming the resistive barriers which act against moving the electrons through the various electric paths, and also against moving the positively charged hydrogen protons through the membrane, and iii) counteracting the mass flow of the reactants (water) and products (oxygen and hydrogen) through the membrane, usually be more noticeable under high current rates and high-pressure conditions. These irreversible behaviors cause voltage drops which are referred to as activation overvoltage, ohmic overvoltage, and concentration or diffusion overvoltage respectively [61]. They are widely and alternatively called overvoltages or overpotentials in the literature. Consequently, the total energy required to start and maintain the electrolysis electrochemical reaction is the sum of energy amounts required to implement the reversible and irreversible processes in this acidic environment. This can be expressed by the following statement:

Total energy consumed = Energy consumed by the reversible action + Energy consumed by the irreversible action.

Thermodynamically, this relation is expressed by (7) where ΔH, the change in enthalpy, indicates the change in the species energy before and after the reaction, ΔG, the change in Gibbs free energy, indicates the energy required by the reversible reaction, and ΔS, the change in entropy, represents the exchange of heat energy caused by the irreversible behavior [52].

$$\Delta H = \Delta G + T\ .\Delta S \quad (7)$$

From this correlation, the energy consumed by the reversible reaction could be used to estimate the reversible voltage required for giving this amount of energy -as calculated in (5)- which is referred to as Gibbs free energy of reaction, the first term in (7). Similarly, the second term ($T\ .\Delta S$) which is the change in entropy of the reaction species could be used to estimate the activation, ohmic, and concentration overpotentials caused by the irreversible action [56]. Various empirical and mathematical models with experimentally fitted parameters are reported in the literature to estimate the activation, ohmic, and concentration overvoltage values to have accurate electrolyzer modeling representations.

3.2. Modeling procedures

In this section, the models implemented by electrical circuit components to emulate the behavior of the electrolyzer will be reviewed and discussed. Electrical models can still be divided according to their development methodology, dynamic behavior, and modeling scale into analytical or empirical models, static or dynamic, and cell or stack, respectively.

3.2.1. Electrical equivalent circuit models of the PEM electrolyzer

Electrical equivalent circuit models (EEC) are the models which use electrical components (e.g., electric voltage and/or current sources, and passive elements: resistors, inductors, capacitors) to construct an electrical circuit that can emulate the behavior of a typical machine or device. For creating an EEC for the PEM electrolyzer, attempts are made to develop such an electrical representation that can emulate the different voltage drops that occur when the electrolyzer is turned on [12,34,35,63–67]. Accordingly, the EEC estimations found in the literature are mainly based on experimental results in the form of polarization curves which are used to develop empirical equations that can closely describe these curves. This section presents a comprehensive analysis and classification of the state-of-the-art equivalent circuit models existing in the literature on PEM electrolyzers. The general equation of the electrolyzer cell voltage is expressed as:

$$E_{cell} = E_{rev} + E_{ohm} + E_{act} + E_{conc/diff} \quad (8)$$

Based on this equation, a general electrical circuit representation could be constructed as depicted in Fig. 3 and used for modeling purposes of the PEM electrolyzer. Each voltage term in this circuit representation might be implemented by a set of electrical circuit elements that may result in a more or less accurate estimation or representation of the real process or activity caused by this voltage drop. Different circuit

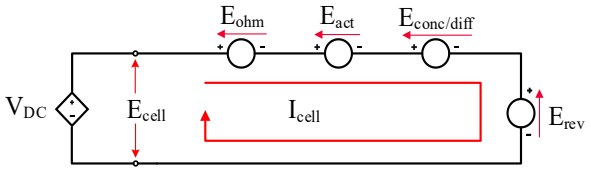

Fig. 3 – General electrical representation of the PEM electrolyzer cell.

models could be generated from this typical circuit representation according to which hypotheses or considerations would be adopted [48,50]. However, in this paper, only these circuit representations proposed in the literature will be discussed and investigated as the aim of this paper is to rearrange and evaluate the existing literature on PEM electrolyzer modeling approaches. Understanding the strengths and challenges of the existing electrolyzer models will help set new ways in motion for improving the overall performance and nicety of these models in emulating the PEM electrolyzer's dynamic behavior [35].

When electrically modeling the PEM electrolyzer, in addition to the reversible and ohmic voltage drops whose effects appear clearly in the polarization curve, there is another effect that needs to be considered, which is the accumulation of charge on both sides of the membrane [57]. This effect is called the double-layer capacitance effect and its leverage is based on both the activation and concentration overvoltage values as explained below.

3.2.2. *Double-layer capacitance effect*

When looking at the electrolysis reaction from an electrical perspective, it can be realized that the accumulation of charge on both sides of the membrane along with the opposite type of charge presented on the electrodes' surfaces results in capacitive effects at the anode and cathode sides of the membrane [33,36]. As a result, in the EEC models, this effect should be emulated by a capacitor component on the anode and cathode sides. In addition, a resistor should be connected in parallel with each of these capacitors to emulate the voltage drop that occurs with this process [57]. The voltage drop associated with the double-layer effect in the electrolyzer is an aggregation of the activation and concentration overvoltage identities. Thus, when combined with the capacitive effect they are usually represented by a parallel RC branch at the anode and cathode to emulate the associated voltage drop as well as the time delay that occurs at each compartment of the electrolyzer cell [57].

3.2.3. *Electrical circuit's voltage components*

Many of the PEM electrolyzer models are built based on calculating the electrical impedance of the electrolyzer cell which is then used to develop the EEC model of the electrolyzer [34,68,69]. In the reported literature on electrical circuit models, it is noted that a dc voltage source is always used to compensate for the effect of the reversible voltage. The ohmic overvoltage is represented by a constant resistor accounting only for the membrane resistance. Nevertheless, the activation and concentration voltage drop terms of the electrolyzer's typical circuit scheme are implemented in different electrical circuit forms. These forms are divided and classified in this paper according to the three main assumptions of the electrolyzer's operating current density (low, moderate, and high current densities).

Fig. 4 shows the schematic circuit diagram of the electrolyzer's electrical impedance models reported in the literature for the PEM electrolyzer modeling. The upper and middle parts of the figure -model (a), and models (b,c)- are built to emulate the electrolyzer behavior in the low and moderate current densities, respectively, and they do not consider the effect of concentration overvoltage. However, the lower part of the figure covers the high current density area and implements the concentration behavior in different forms as depicted in models (d, e, and f).

Brief explanations of the electrical circuit's voltage components and their associated considerations and hypotheses are presented in the subsections below.

3.2.3.1. Reversible voltage. Reversible voltage is the voltage consumed by the reversible reaction and is responsible for the production of hydrogen [31,70,71]. This voltage inherently changes with the change in operating temperature and pressure of the cell, however in the EEC models, it is assumed to be constant and emulated by a constant DC voltage generator or a battery component as revealed by the following equation [33,36]:

$$E_{rev} = V_{int} \tag{9}$$

The amount of electrical power converted into hydrogen can be simply calculated as the product of the reversible voltage and the electric current passing through the electrolyzer terminals as expressed by (10) [48]:

$$P_{elect,\,H_2} = E_{rev} \cdot I_{cell}(t) \tag{10}$$

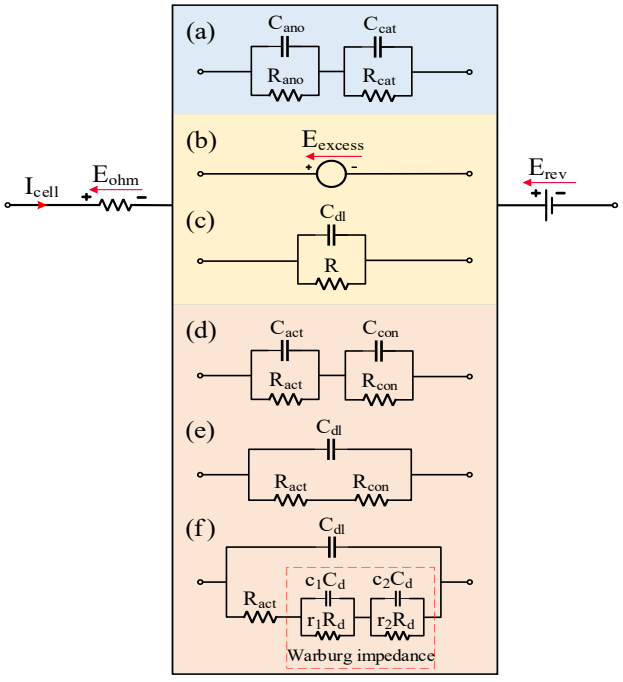

Fig. 4 – Schematic circuit diagrams of the electrical models reported in the literature of PEM electrolyzer modeling.

Nevertheless, for a more accurate estimation of the amount of power converted into hydrogen as well as the total efficiency of the electrolyzer cell, the reversible voltage should be represented by its variable nature based on the operating temperature and pressure of the electrolyzer cell as approximated by the next equations:

$$E_{rev} = E_{rev}(T,P) = E_{rev}(STP) + \frac{RT}{n_{H_2}F}\ln\left(\frac{P_{H_2}\cdot\sqrt{P_{O_2}}}{a_{H_2O}}\right) \quad (11)$$

$$E_{rev} = E_{rev}(T,P) = E_{rev}(STP) + \frac{RT}{n_{H_2}F}\ln\left(\frac{P_{output}}{P_{Input}}\right) \quad (12)$$

Reference [57] reported that the increase in temperature decreases the reversible voltage while the change in pressure has a negligible effect on the reversible voltage. Therefore, in electrical circuit modeling, the reversible voltage is usually emulated by a constant voltage source as shown in (9). Table 2 presents a summary of the reversible voltage equations used in the electrical circuit modeling literature of the PEM electrolyzer.

3.2.3.2. *Ohmic overvoltage*. Ohmic overvoltage is a representation of the energy lost due to all the resistive barriers acting against the movement of electric charge carriers through the different paths of the electrolysis cell. Therefore, the total ohmic resistance of the ohmic overvoltage is the accumulation of ohmic resistances due to the electronic current collectors, catalyst layers, the electrolyte membrane, and the contact resistances of all these plates [75]. As mentioned in the physical modeling approach, three different considerations can be followed when it comes to calculating the ohmic resistance of the electrolysis cell [50]. However, in the EEC modeling (exactly like in the physical modeling approach), the electrical part of the resistance is usually neglected and only the resistance of the electrolytic membrane would be considered [58,60,69,75–79]. Therefore, throughout the consulted literature, the ohmic voltage drop is emulated by a series resistor to represent the electrical resistance of the membrane and amount of voltage drop that occurs across it as shown in Fig. 4.

$$E_{ohm} = R_{ohm} \cdot I_{cell}(t) \quad (13)$$

3.2.3.3. *Activation overvoltage*. From the electrical perspective, the activation overvoltage is there to emulate two main actions, the first one is the influence of the resistive barriers that need to be overcome to free up electrons from the surfaces of charged electrodes which is called the charge transfer resistance. While the second one is to account for the time delay wasted by the accumulated charge (on both sides of the polymeric membrane) in the anode and cathode to vary upon variation of the electrolyzer's current [33,59,80]. Therefore, a resistor element is needed to emulate the heat loss or heat energy consumed by the reaction to free electrons up from the electrode surfaces as well as a capacitor element to emulate the accumulation of charge and time needed due to its variation upon current variation. To this end (and as stated previously in the explanation of the double-layer capacitance effect), a parallel RC branch could be used to emulate the whole action and it can be repeated separately at the anode and cathode sides of the electrolyzer as they have different speeds of reaction [33,36,67]. Nevertheless, different assumptions can be considered to interpret how the activation overvoltage is implemented in the EEC models as follows:

1. At low current densities, when the effect of concentration overvoltage is neglected, two series-connected RC branches could be used to emulate the activation voltage drop of the anode and cathode compartments separately, see Fig. 4 part (a).
2. At moderate current densities, it can be emulated in combination with the concentration overvoltage either by:
   (a) an excess voltage drop component in a static equivalent circuit model, see Fig. 4 part (b).
   (b) a single RC branch in the circuit to emulate the overall behavior of the anode and cathode compartments together, see Fig. 4 part (c).
3. At high current densities, the activation overvoltage is usually represented by a resistor connected in series with the concentration overvoltage's circuit components, and the group is connected in parallel with the double-layer capacitor in a bigger RC branch as shown in Fig. 4 parts (e and f).

The mathematical equations from these assumptions and their associated circuits can be expressed as follows:

1. When a static model is considered, the activation overvoltage may be either neglected or expressed as an excess voltage drop and it can be expressed by one of the next two equations [38,39]:

$$E_{act} = \eta_{act,ano} + \eta_{act,cat} = 0 \quad (14)$$

$$E_{act} = \eta_{act,ano} + \eta_{act,cat} = I_{cell} \cdot [E_{cell} - V_{int}] = 1.476\, e^{-\frac{5}{0.02} I_{cell}} \quad (15)$$

2. When expressed by a single RC branch in a dynamic model (estimation of this equation is provided in the Appendix) [33,36,64].

$$E_{act}(t) = \left(\frac{\tau}{C}\right) \cdot \left(L^{-1}\left[\frac{1}{(\tau s+1)} \cdot \int_0^{\infty} I_{cell}(t) \cdot e^{-st} \cdot dt\right]\right) + E_{act}(0) \cdot e^{-\frac{t}{\tau}} \quad (16)$$

3. When expressed by two RC branches in a dynamic model [33,36].

$$\left.\begin{aligned} &E_{act}(t) = \eta_{act,ano} + \eta_{act,cat} \quad where, \\ &\eta_{act,k} = \left(\frac{\tau_k}{C_k}\right) \cdot \left(L^{-1}\left[\frac{1}{(\tau_k s+1)} \cdot \int_0^{\infty} I_{cell}(t) \cdot e^{-st} \cdot dt\right]\right) + \eta_{act,k}(0) \cdot e^{-\frac{t}{\tau_k}} \end{aligned}\right\} \quad (17)$$

Table 2 – Equations of reversible voltage in the electrical circuit models of the PEM electrolyzer.

Reversible overvoltage	ID	Refs.
$E_{rev} = V_{int}$	REV I	[33,36]
$E_{rev} = E_{rev}(T,P) = E_{rev}(STP) + \frac{RT}{n_{H_2}F}\ln\left(\frac{P_{H_2}\cdot\sqrt{P_{O_2}}}{a_{H_2O}}\right)$	REV II	[50,52,72]
$E_{rev} = E_{rev}(T,P) = E_{rev}(STP) + \frac{RT}{n_{H_2}F}\ln\left(\frac{P_{output}}{P_{Input}}\right)$	REV III	[48,73,74]

4. When expressed as a series resistance with mass transfer resistance in a parallel RC branch as in Fig. 4 part (e).

$$E_{act} = \left(\frac{R_{act}}{R_{act} + R_{mass}}\right) \cdot E_{total} \tag{18}$$

In this last equation E_{total} is the overall voltage of the bigger RC branch containing the components of the activation and concentration overvoltage and it may be expressed as follows:

$$E_{total}(t) = \left(\frac{\tau_{tot}}{C_{dl}}\right) \cdot \left(L^{-1}\left[\frac{1}{(\tau_{tot}s+1)} \cdot \int_0^{\infty} I_{cell}(t) \cdot e^{-st} \cdot dt\right]\right) + E_{total}(0) \cdot e^{-\frac{t}{\tau_{tot}}} \tag{19}$$

Table 3 provides a summary of the equations mentioned in this section to determine the activation overvoltage.

3.2.3.4. Concentration or diffusion overvoltage. As the mathematical equations, on which the electrical circuit models are based, are originally empirical equations derived from the polarization curves drawn from real experimental results, it is noticed in many cases that the effects of activation and concentration overvoltage have usually been linked with each other and with the double-layer capacitance effect. In other words, when derived from the polarization curve, their influences cannot be separated from each other as they both share in the double-layer capacitance effect [13,22,37,63,84]. Moreover, activation and concentration voltage drops are very similar to the extent that they are even derived from the same general equation in the physical modeling approach (Butler-Volmer's equation). Similarly, in EEC models, they are in most cases joined under one boundary but still expressed by separate components [12,19,35]. Similar to its activation counterpart, the concentration overvoltage may be modeled in different forms according to several assumptions that can be stated as follows:

1. At low current densities, the concentration overvoltage could be neglected as the diffusion process is not considered to be a limiting process, and thus only the activation overvoltage is considered in the circuit representation as shown in Fig. 4 part (a).
2. At moderate current densities, the concentration voltage drop is linked to the activation voltage drop and emulated by one excess voltage term as found in the static or steady-state equivalent circuit models, see Fig. 4 part (b).
3. At high current densities, the concentration overvoltage can be emulated either by:
   (a) A resistor in series with the resistor of the activation overvoltage in a single RC branch, see Fig. 4 part (e).
   (b) A single RC branch, for both anode and cathode, connected in series with the activation resistor in a larger RC branch.
   (c) A separate RC branch, for both of anode and cathode, connected in series with the RC branch of the activation overvoltage, see Fig. 4 part (d).
   (d) Two separate RC branches for the anode and cathode are connected in series with each other and with the activation resistor in a larger RC branch, see Fig. 4 part (f).

The concentration/diffusion losses could be estimated by the Warburg impedance as part of the Randles-Warburg impedance estimation which is widely accepted to model either the galvanic or electrolytic cells [68]. Further, the Warburg impedance can be approximated by an RC branch and that is why this approximation is used here for representing the concentration overvoltage [85]. When modeled, the concentration overvoltage may be mathematically expressed by one of the following equations:

1. At low current densities and when a static model is assumed.

$$E_{conc/diff} = \eta_{conc,ano} + \eta_{conc,cat} = 0 \tag{20}$$

2. When expressed as a series resistance.

$$E_{conc/diff} = \eta_{conc,ano} + \eta_{conc,cat} = \left(\frac{R_{mass}}{R_{act} + R_{mass}}\right) \cdot E_{total} \tag{21}$$

3. When expressed with a single RC branch.

$$E_{conc}(t) = \left(\frac{\tau_{conc}}{C_{conc}}\right) \cdot \left(L^{-1}\left[\frac{1}{(s\tau_{conc}+1)} \cdot \int_0^{\infty} I_{cell}(t) \cdot e^{-st} \cdot dt\right]\right) + E_{conc}(0) \cdot e^{-\frac{t}{\tau_{conc}}} \tag{22}$$

4. When expressed with two separate series RC branches (Warburg).

$$\left.\begin{aligned} E_{conc/diff} &= \eta_{conc,ano} + \eta_{conc,cat}, \\ \eta_{conc,k} &= \left(\frac{\tau_k}{C_k}\right) \cdot \left(L^{-1}\left[\frac{1}{(\tau_k s+1)} \cdot \int_0^{\infty} I_{cell}(t) \cdot e^{-st} \cdot dt\right]\right) + \eta_{conc,k}(0) \cdot e^{-\frac{t}{\tau_k}} \end{aligned}\right\} \tag{23}$$

Table 3 – Equations of activation overvoltage in the electrical circuit models of the PEM electrolyzer.

Activation overvoltage	ID	Refs.
$E_{act} = \eta_{act,ano} + \eta_{act,cat} = 0$	*ACT I*	[67]
$E_{act} = \eta_{act,ano} + \eta_{act,cat} = I_{cell} \cdot [e_{rev} - V_{int}] = 1.476\, e^{-\frac{5}{0.02} I_{cell}}$	*ACT II*	[38,39,65,81–83]
$E_{act}(t) = \left(\frac{\tau}{C}\right) \cdot \left(L^{-1}\left[\frac{1}{(\tau s+1)} \cdot \int_0^{\infty} I_{cell}(t) \cdot e^{-st} \cdot dt\right]\right) + E_{act}(0) \cdot e^{-\frac{t}{\tau}}$	*ACT III*	[66,69]
$E_{act}(t) = \eta_{act,ano} + \eta_{act,cat}$ *where,* $\eta_{act,k} = \left(\frac{\tau_k}{C_k}\right) \cdot \left(L^{-1}\left[\frac{1}{(\tau_k s+1)} \cdot \int_0^{\infty} I_{cell}(t) \cdot e^{-st} \cdot dt\right]\right) + \eta_{act,k}(0) \cdot e^{-\frac{t}{\tau_k}}$	*ACT IV*	[33,36,59,60,67,80]
$E_{act} = \left(\frac{R_{act}}{R_{act} + R_{mass}}\right) \cdot E_{total}$	*ACT V*	[35,63,84]

Or it can be calculated using the Warburg impedance (Fig. 4 part (f)) that can be approximated by the following transfer function:

$$Z_{wbg}(s) = R_d\left(\frac{\tanh\sqrt{s\tau_d}}{\sqrt{s\tau_d}}\right) \approx R_d\left(\frac{r_1}{(r_1c_1\tau_d)s+1} + \frac{r_2}{(r_2c_2\tau_d)s+1}\right) \forall \tau_d = R_dC_d \quad (24)$$

r_1, r_2, c_1, c_2 are the dimensionless Warburg coefficients of the four circuit components ($r_1R_d, r_2R_d, c_1C_d, c_2C_d$) constituting the Warburg impedance. These coefficients are estimated by fitting the left and right sides of (24) using the Levenberg-Marquardt algorithm [68]. R_d, τ_d are the diffusion resistance and diffusion time constant respectively. C_d is the diffusion capacitance. Table 4 presents a summary of the equations discussed in this section to calculate the concentration overvoltage.

3.2.4. *Other electrical models*

The model proposed in Ref. [86] assumes that the power consumption of the electrolysis cell is proportional to the squared difference of the cell and water dissociation reversible potentials. This premise can be expressed mathematically by the following equation:

$$P_{cell} \propto (E_{cell} - E_{rev})^2 \quad (25)$$

where P_{cell} is the amount of power consumed in the electrolyzer cell and it is greater than the power required for the water dissociation reaction, E_{cell} and E_{rev} are the cell and reversible voltage values respectively. A more practical version of this relation could be found by accounting for the effects of ohmic voltage drop that occur due to the resistance of the electrodes, electrolyte (i.e., membrane), and the interfacial/contact surfaces in the membrane-electrode assembly. When current I_{cell} passes through the electrolyzer terminals, the voltage drop and electric power consumed because of the total ohmic resistance can be expressed as [86]:

$$\left.\begin{aligned} E_{ohm} &= I_{cell}R_{ohm} \\ P_{ohm} &= (I_{cell})^2 R_{ohm} \\ P_{cell} &= I_{cell} \cdot E_{cell} \end{aligned}\right\} \quad (26)$$

By substituting (26) in (25), a relation of the excess power consumed in the electrolyzer cell can be estimated as in (27) below:

$$\left.\begin{aligned} P_{excess} &= P_{cell} - P_{ohm} \propto (E_{cell} - E_{ohm} - E_{rev})^2 \\ P_{excess} &= \left(I_{cell} \cdot E_{cell} - (I_{cell})^2 R_{ohm}\right) \propto (E_{cell} - I_{cell}R_{ohm} - E_{rev})^2 \end{aligned}\right\} \quad (27)$$

Changing the proportionality by an equal sign and a proportional constant K yields:

$$\left(I_{cell} \cdot E_{cell} - (I_{cell})^2 R_{ohm}\right) = K \cdot (E_{cell} - I_{cell}R_{ohm} - E_{rev})^2 \quad (28)$$

Table 4 – Equations of concentration overvoltage in the electrical circuit models of the PEM electrolyzer.

Concentration/diffusion overvoltage	ID	Refs.
$E_{conc/diff} = \eta_{conc,ano} + \eta_{conc,cat} = 0$	*Conc I*	[33,36,60,67,80]
$E_{conc/diff} = \eta_{conc,ano} + \eta_{conc,cat} = \left(\frac{R_{mass}}{R_{act} + R_{mass}}\right) \cdot E_{total}$	*Conc II*	[35,63,84]
$E_{conc/diff}(t) = \left(\frac{\tau_{conc}}{C_{conc}}\right) \cdot \left(L^{-1}\left[\frac{1}{(s\tau_{conc}+1)} \cdot \int_0^{\infty} I_{cell}(t) \cdot e^{-st} \cdot dt\right]\right) + E_{conc}(0) \cdot e^{-\frac{t}{\tau_{conc}}}$	*Conc III*	[66,69]
$E_{conc/diff} = \eta_{conc,ano} + \eta_{conc,cat}$ *where,* $\eta_{conc,k} = \left(\frac{\tau_k}{C_k}\right) \cdot \left(L^{-1}\left[\frac{1}{(\tau_k s+1)} \cdot \int_0^{\infty} I_{cell}(t) \cdot e^{-st} \cdot dt\right]\right) + \eta_{conc,k}(0) \cdot e^{-\frac{t}{\tau_k}}$	*Conc IV*	[12,19,34,68,76,85]
$E_{conc/diff} = I_{cell} \cdot Z_{wbg}$	*Conc V*	[19,68,85]

The constant K is referred to as the coefficient of power conversion which acts as an indication of the electrolytic cell's capability to convert electricity into chemical energy, and it is different for different electrolytic cells and operating conditions. The unit of the power conversion coefficient is ohm^{-1} (Ω^{-1}) although it has no relation to the resistivity or conductivity of the electrolytic cell. Rearranging (28), the relation between the current and voltage of the electrolysis cell could be expressed as:

$$I_{cell} = \frac{E_{cell} + 2KR_{ohm}\,(E_{cell} - E_{rev}) - \sqrt[2]{(E_{cell})^2 + 4KR_{ohm}E_{rev}\,(E_{cell} - E_{rev})}}{2R_{ohm}\,(1 + KR_{ohm})} \tag{29}$$

The current-voltage characteristics of the electrolysis cell expressed by (29) vary with the variation of three parameters K, R_{ohm}, E_{rev}. The value of E_{rev} is the voltage needed by the water decomposition reaction and it determines the starting point of the cell polarization curve. The value of resistance R_{ohm} determines the slope of the characteristic (i.e., polarization) curve while the value of the power conversion coefficient K affects both the slope and envelope of the curve and it falls in the range $(0 \leq K \leq \infty)$.

When $K = 0$, the current in the electrolytic cell will vanish ($I_{cell} = 0$) as no electric current will pass through the cell and no electrochemical reaction would happen if the electrodes had no kinetic activities. On the contrary, when $K \rightarrow \infty$, (29) shrinks to:

$$I_{cell} = \frac{(E_{cell} - E_{rev})}{R_{ohm}} \tag{30}$$

This equation represents a straight line that passes through the point (E_{rev}, 0) and has a slope equal to $\frac{1}{R_{ohm}}$. This means that when the electrodes are kinetically active in an infinite way, the electrochemical cell acts as a pure resistance, and its polarization curve will be represented by a straight-line graph.

3.3. *Validation methods of electrolyzer models*

Validation of the electrical circuit models is mainly conducted by comparing the model results against those of the electrolyzer experimental tests. The accuracy of the model in replicating the static and dynamic behavior of the electrolyzer revealed by the experimental setup greatly depends on the model parameters which are usually obtained through the implementation of curve-fitting techniques. In other words, the accuracy and efficiency of the used curve fitting method will be directly reflected in the accuracy and efficacy of the model in replicating the electrolyzer behavior [59,60,87–89]. Therefore, other parameterization techniques need to be developed to accurately estimate and validate the behavior of the electrical circuit models.

4. Discussion

This paper provides an extensive review of the electrical circuit models proposed in the literature on PEM electrolyzers in the last 15 years. The electrical models of PEM electrolyzers are reported in the literature under different assumptions and working conditions. However, in this paper, these models have been aggregated to accentuate the differences and similarities between them. This section presents a brief yet comprehensive discussion of the models in terms of comparisons of their simulation results as well as their applications, benefits, and shortcomings derived from the reported papers in the literature.

4.1. *Simulation of electrolyzer models*

The electrolyzer models reviewed in this paper have been implemented in MATLAB/SIMULINK environment and the results are compiled to demonstrate how the models behave in relation to the unit cell voltage and dynamic behavior in response to a gradual and sudden changes in input current, respectively. Fig. 5 shows the voltage-current characteristics of the implemented models. It can be noted in Fig. 5 that all simulated models have the same starting point where they intersect with the vertical axis, this voltage value is the reversible voltage, and it is common between all models. Nevertheless, as the input current of the electrolyzer cell increases, the cell voltage of the different models starts to deviate, and this deviation increases as the current increase.

When the cell current attains a value of 50 A, which represents a current density of 0.0833 A/cm^2 for a 0.06 m^2 cell, the difference between the lowest value (about 21.6 V attained by models b, e) and the highest value (close to 29.6 V attained by model f) of the cell voltage will be of the order of 8 V which is not a small difference for this value of current density (see the zoomed part of Fig. 5). As the cell current continues to increase as in Fig. 5, the difference between the highest and lowest voltage value continues to increase and it reaches 17.5 V as the current reaches 100 A for a current density of 0.167 A/cm^2.

Fig. 6 shows the activation overvoltage part of the cell voltage as produced by four circuit representations over the current range 0–50 A. When the current is zero, the activation overvoltage of all models equals zero and starts to increase at the moment when the current is initiated in the electrolysis cell. However, the rate at which this voltage increase differs from one model to another. The activation overvoltage emulated by models b and c increases linearly with the current, but that of models a and e encounters some delay and slower change rate due to the presence of capacitor components that emulate the non-instant change of charge accumulation, on the anode and cathode sides, with change in current.

The dynamic behavior of the electrical circuit models under investigation is tested and depicted in Fig. 7 to compare the dynamic characteristics of the reported electrolyzer models with sudden changes in the electrolyzer current. In part (a) of Fig. 7, the current changed from 0 to 5 A at time t = 2 s and from 5 to 15 A at time t = 40 s. For a step change of 5 A in the current, on one hand, the static model b showed an instant change in the electrolyzer voltage. On the other hand, models f and c showed a transient response and reached steady-state after small time constants of about 1.5 s and 2 s respectively. Models a and e showed much slower dynamics and reached their steady state after around 33 s of the current change as depicted in Fig. 7 (b). With a closer look at Figs. 5–7,

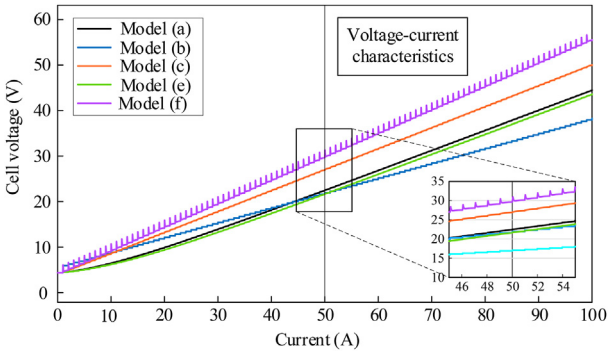

Fig. 5 – Voltage-current characteristics of the various electrolyzer circuit representations.

it can be noted that models a and e exhibit very close and similar behaviors either with the gradual or sudden change of the input current.

To sum up, the electrical circuit models of the electrolyzer have some similarities as well as differences. For example, all models exhibited quite linear voltage-current characteristics despite the divergent slopes. However, they showed dissimilar dynamics with the step change in current as well as a clear mismatch in their steady-state voltage values. Therefore, more investigations are required to decrease the discrepancy between these models as well as to improve their accuracy in emulating the static and dynamic behavior of the electrolysis cell.

In the remainder of this section, a comparison is carried out to the research papers reported in the literature that adopted electrical circuit models in their implementations and the results are shown in Table 5 and Table 6.

Table 5 categorizes each study based on the objective, modeling scale, and dynamic behavior exhibited by the implemented electrolyzer model. It can be seen that the majority of models are developed for describing the performance of one cell and fewer models are considered to describe the electrolyzer stack as one unit. Although its characteristics are approximated based on the number of cells it may comprise. Similarly, in Table 6, the published research papers are categorized according to the modeling scale, type of model, and

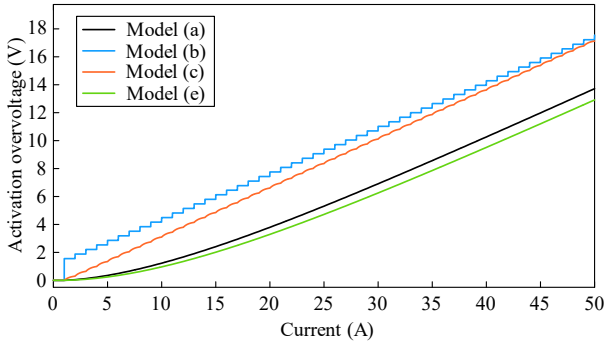

Fig. 6 – Activation overvoltage emulated by different electrical circuit models.

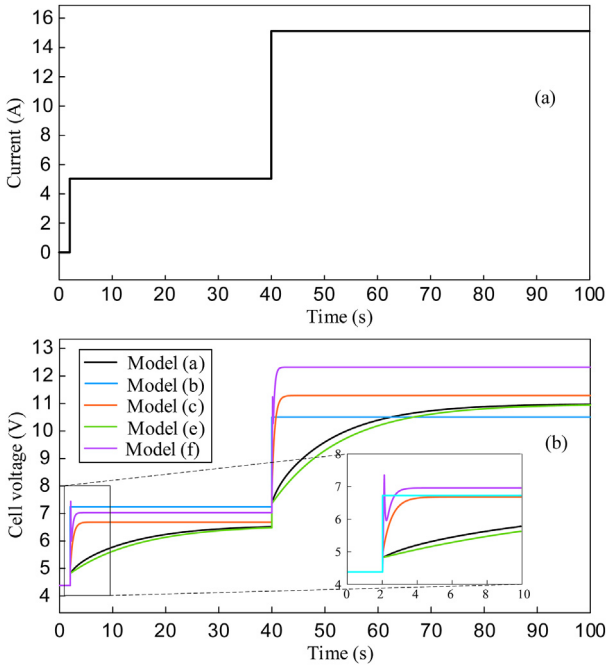

Fig. 7 – Dynamic behavior of the electrolyzer models with a sudden change in the input current: (a) change in cell current, (b) transient response of the cell voltage.

the purpose of study or targeted objectives. Models a,b,c,d,e, and f mentioned in Table 6 refer to those equivalent electrical circuit representations shown in Fig. 4.

4.2. *Applications of electrical equivalent circuit modeling for design and analysis of PEM electrolyzer*

As mentioned previously, electrolyzers are to be fed by cheap electricity from RESs. Electrolyzers cannot be connected directly to the output of RESs, power electronics converters have to act as an intermediate stage to make the electrolyzer operation more efficient. Meanwhile, electrical circuit models play an inevitable role in the design and analysis of the different system components and associated control techniques. In Ref. [64], an electrical circuit model of the electrolyzer is used to analyze the response of a mega-scale electrolyzer stack to step changes in the grid frequency. The study revealed that the electrolyzer responds to grid frequency changes faster than traditional generators. Electrical circuit models are also used in Ref. [13] to investigate the ancillary services and the virtual inertia response that electrolyzers can provide by implementing a virtual synchronous machine control approach on the electrolyzer system.

Based on the information collected from the literature, the choice of the electrical model to be used for a study depends greatly on the application of the study itself, for example, it is noted that when the electrolyzer is integrated into grid-connected applications, a static model is usually used for modeling the electrolyzer as the amount of generated hydrogen and operational efficiency are the parameters of interest in this case. On the other hand, when the electrolyzer

Table 5 – Research papers included electrical circuit representation for modeling the PEM electrolyzer.

Year	Study objective	Modeling scale	Model behavior	Outcomes	Limitations	Refs.
2023	System modeling, performance assessment.	Cell	Static	Electrolyzer efficiency increases with increasing temperature and decreases with increasing pressure.	A static model is used to analyze the electrolyzer performance with an energy plant which is a dynamic source. Thermal and mass transfer effects are neglected.	[41]
2023	Investigate electrolyzer models, power converters, and control approaches.	Cell	_____	An overview of the electrolyzer models, suitable converters, and control approaches is provided.	Several models and assumptions are uncovered.	[40]
2023	Providing primary and frequency control and virtual inertia response.	Stack	Dynamic	Electrolyzers are suitable candidates for virtual inertia provision in future grids.	The monolithic construction of the electrolyzer leads to inconveniences between frequency control provision and hydrogen downstream production.	[13]
2022	Improving the efficiency of a hybrid microgrid.	Cell	Static	Improved efficiency, Load demand always satisfied.	A static model is used with the solar PV system which is a dynamic system, thermal and mass transfer effects are neglected.	[38]
2022	Studying the performance of an electrolyzer/fuel cell/ battery energy storage system.	Cell	Static	The hybrid system provided better performance than battery-only systems. Provide higher energy density and lower specific energy consumption.	The system has a high initial cost and is not beneficial economically except for remote areas.	[39]
2022	Providing flexible system control strategy to provide frequency reserve in smart grids.	Stack	Dynamic	The electrolyzer has been used in a formic acid generation plant to help provide frequency services to the grid.	The provided power reserve is limited by the capacity of system compressors.	[12]
2021	Using electrolyzers to provide grid active and reactive power control and ancillary services.	Cell	Dynamic	Increasing the size of the electrolyzer plant increases its dynamic operational range. The power electronic interface can help mitigate these dynamic changes.	No feedback signals from the electrolyzer have been used in the control loops of the power converter controlling the electrolyzer.	[37]
2020	Proposing large-scale electrolyzers for grid frequency support.	Stack/Cell	Dynamic	Electrolyzers have a positive effect on frequency stability, they respond to frequency deviations faster than conventional generators.	Thermal and mass transfer effects are neglected.	[34,35]
2020	Developing a static-dynamic model of the electrolyzer to study performance characteristics.	Cell	Dynamic	The input current ripples can degrade the cell's performance. Degradation and wear effects result due to dynamic operating conditions from coupling with RESs.	The model produces some errors in modeling the dynamic behavior when tested against experimental results.	[33,36]

is considered for providing voltage/frequency grid support and ancillary services, the dynamic model will be a more suitable choice for conducting the study.

Electrolyzer applications can be divided into three main areas:

1. Grid-fed water electrolysis for versatile gas applications.
2. Hybrid microgrid-based water electrolysis for remote power applications.
3. Renewable energy-based water electrolysis for mass production of green hydrogen.

Table 6 – Review of the different model representations proposed for the PEM electrolyzer.

Year	Modeling scale	EECM	Purpose of the study/Model application	Refs.
2023	Stack	Model (c)	Providing grid ancillary services	[13]
2022	Cell	Model (b)	Performance analysis	[38,39,65]
2022	Cell	Model (f)	Performance analysis	[19]
2022	Cell	Model (c)	Providing grid ancillary services	[64]
2022	Stack	Model (f)	Providing grid ancillary services	[12]
2022	Stack	Model (a)	Modeling & characterization	[59,67,80]
2022	Cell	Model (d)	Parameters identification	[66]
2021	Cell	Model (a)	Modeling & characterization	[36]
2021	Cell	Model (c)	Providing grid ancillary services	[37]
2021	Stack	Model (e)	Providing grid ancillary services	[63]
2021	Stack	Model (c)	Providing grid ancillary services	[73]
2020	Stack	Model (a)	Modeling & characterization	[33]
2020	Cell	Model (f)	Providing grid ancillary services	[34]
2020	Stack	Model (e)	Providing grid ancillary services	[35]
2020	Cell	Model (d)	Parameters identification	[69]
2019	Cell	Model (c)	Modeling & characterization	[22]
2019	Cell	Model (a)	Modeling & characterization	[60]
2018	Stack	Model (e)	Providing grid ancillary services	[84]
2014	Cell	Model (f)	Modeling & characterization	[68]
2013	Cell	Model (f)	Modeling & characterization	[76,85]
2011	Cell	Model (c)	Providing grid ancillary services	[18]
2011	Cell	Model (b)	Modeling & characterization	[82,83]
2009	Cell	Model (b)	Modeling & characterization	[81]

Therefore, the dynamic behavior of the electrolyzer models can accordingly be classified as static, static-dynamic, and dynamic, respectively.

If the electrolyzer plant is fed from the grid, a continuous and relatively constant voltage will be supplied to the electrolyzer. Thus, a static model may be more suitable to model the electrolyzer behavior in this case as it will be working in a continuous mode from a stable power supply. However, when it is connected to a micro- or mini-grid with hybrid sources, or when it is connected to an islanded microgrid, a dynamic model may be then required to allow capture of the interaction between the electrolyzer plant and other grid components. Table 7 lists the applications into which the electrolyzer may be integrated with a power source. It also indicates the type of behavior the model can have and lists the parameters of interest for each application.

As it is just elaborated, the application and parameters of interest greatly help choose which type of behavior is more likely to have and accordingly which model should be chosen to emulate the electrolyzer action. Fig. 8 shows the schematic diagrams of the electrolyzer applications discussed above and mentioned in Table 7. It is obvious from Tables 5–7, and Fig. 8 that the application of electrical circuit models is widely used to design, analyze, and evaluate the behavior as well as the performance parameters of the electrolyzer. This implies how important these models are and highlights the fact that their enhancement is a milestone in the transition to hydrogen-dominated fuel and energy markets.

4.3. *Benefits and shortcomings of electrolyzer electrical circuit modeling*

Electrolyzer EEC, as any electrical circuit of any other electrical device or machine, is of great importance in the design, analysis, and evaluation of the electrolyzer's operation. In addition to allowing accurate modeling, it promotes a better design, organization, testing, monitoring, and analysis of the electrolyzer behavior in a very cost-effective way. Further, working on the electrical models of the electrolyzer can help in understanding the phenomena happening inside the device plus analyzing the electrolyzer operation under different operating scenarios without sacrificing the actual expensive

Table 7 – Applications and parameters of interest for PEM electrolyzer's model behaviors.

Model behavior	Application	Parameters of interest	Modeling scale
Static	Grid-fed electrolyzer plant or hydrogen energy hub for versatile gas applications.	Operating efficiency. Hydrogen production. Specific energy consumption.	Cell/Stack
Static-dynamic	Hybrid microgrid-fed electrolyzer plant for remote areas' power and gas applications.	Operating efficiency. Voltage/frequency support. Grid ancillary services.	Cell/Stack
Static-dynamic	Renewable energy-based electrolyzer plant for mass production of green hydrogen.	Operating efficiency. Plant operational and safety constraints. Mass production of hydrogen.	Stack

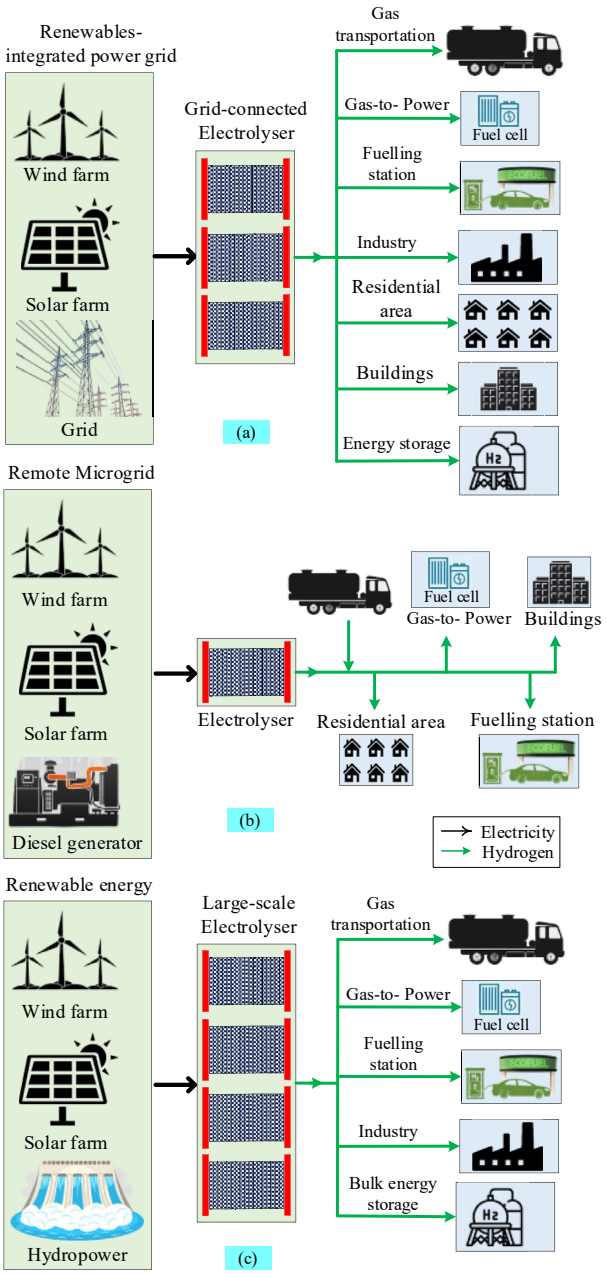

Fig. 8 – Applications of PEM electrolyzer for hydrogen production: (a) grid-fed electrolyzer, (b) remote microgrid-fed electrolyzer, and (c) renewable energy-based electrolyzer.

device. With the electrical circuit model, it is much easy to vary the circuit parameters and even try new circuit components which may be physically impossible, it allows testing of an unlimited number of values for the different circuit variables and components in order to understand and improve the circuit behavior.

Moreover, electrical circuit models are easier to construct and control than fluidic, physical, or thermal models. Another benefit is the safety of man and machine as these models can

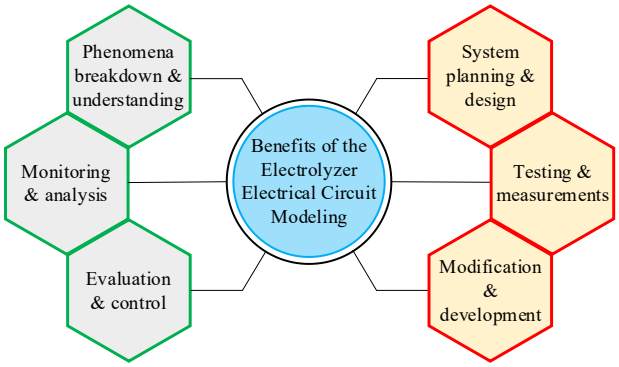

Fig. 9 – Benefits of the electrolyzer's electrical circuit modeling.

hold zero or negligible hazards to the man working on them. Fig. 9 represents a visualization of the benefits of the electrolyzer electrical circuit modeling.

On the other hand, one of the main shortcomings of electrolyzer's electrical circuit models is that all of the models are derived and developed based on experimental data using curve fitting methods. Consequently, the parameters of these models usually reflect the specific conditions in which these experiments are conducted. However, since the dynamics of the electrolysis cell change with the change in operating conditions like temperature and pressure, the development of models with adaptive parameters is highly recommended [49]. Another shortcoming is that yet there is no systematic procedure to follow to aggregate the electrical circuit models in order to develop descriptive models of large-scale stacks or electrolyzer plants with series and parallel connections. One more thing is that the electrical circuit models do not have any circuit components to emulate the degradation of the electrolyzer cells due to prolonged operation and the current ripple imposed by power electronics devices [36]. This again highlights the need for more sophisticated models and controls with more monitoring and diagnostics capabilities.

5. Challenges in the development and application of PEM electrolyzer modeling

5.1. *Intermittency of RESs*

When powered by RESs, the PEM electrolyzer plant will be affected by the intermittency of these resources which in turn adversely affect their operation and working efficiency. Furthermore, this fluctuating operation leads to degradation in the performance of the electrolyzer's internal components like the current collector and catalyst plates. This degradation greatly reduces the productivity and purity of hydrogen production and shortens the lifetime of the device [90,91]. As the demand for hydrogen is expected to increase significantly in the near future, reliable operation of the electrolyzer needs to be achieved through the implementation of sophisticated power electronics controls and energy coordination strategies

to help mitigate the effect of resource irregularity in the grid [92]. Moreover, advancements in material science can greatly improve the electrolyzer performance by introducing new materials that can be less expensive with higher deterioration resistivity to be used in the manufacturing of new internal electrolyzer plates.

5.2. *Series-parallel connection*

As revealed in the reported literature, when aggregated in series and parallel combinations, the electrolyzer cells and stacks are usually treated the same as connecting resistive loads in series and parallel combinations. Thus, if all cells in the stack are connected in series, the total voltage of the stack is equal to the sum of the voltages of all cells, whereas if they are connected in parallel, it is equal to the voltage of one cell. However, the electrodes in the electrolyzer cells can be connected in a monopolar or bipolar configuration, then these cells will be connected in series or parallel which may thus result in different connection considerations to be taken into account when calculating the total stack voltage and current ratings [93]. Fig. 10 shows the monopolar and bipolar connection of the electrodes in the electrolyzer cells.

According to the authors in Ref. [94], the total faradaic current, which is responsible for the production of hydrogen, of the electrolyzer stack is always equal to the sum of the faradaic currents of the individual cells, regardless of whether they are connected in series or parallel. It is because the total number of electrons transferred to hydrogen in a stack is equal to the number of cells in the stack multiplied by the

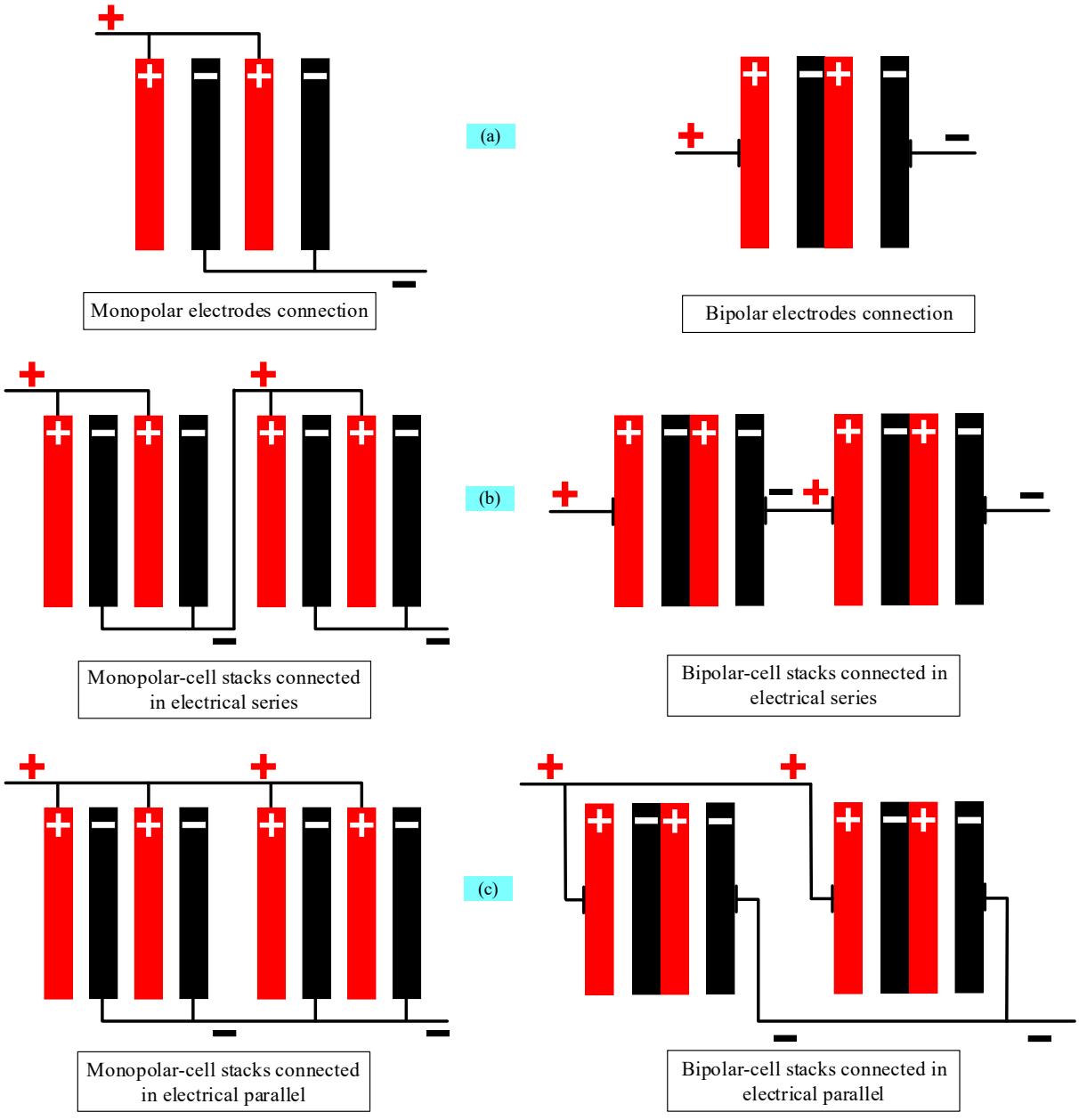

Fig. 10 – Monopolar and Bipolar cell connections: (a) inter-cell electrodes connection, (b) series-connected stacks, and (c) parallel-connected stacks.

number of electrons transferred to hydrogen in each cell. It is also possible for leakage and reverse currents to occur in the circuitry of the connected cells/stacks. Therefore, further research on the series-parallel connection is required to develop more accurate, reliable, and descriptive models for the PEM electrolyzer.

5.3. *Scalability*

When scaling-up electrolyzers, special attention should be taken if either these electrolyzer modules or stacks will be connected in parallel to the same DC source or if each module will be connected to a separate source, i.e., where these sources are assumed to be in the form of DC power converters. In the first scenario, the converter output voltage should be shared equally between the connected electrolyzers to avoid unequal sharing of power which may result in circulating currents or variable hydrogen production at the electrolyzer output which may affect the stability and accuracy of the monitoring and control devices as well as adversely affect other balance-of-plant devices. In the second scenario, equal amounts of power should still be assured if the system consists of identical converters feeding identical electrolyzer modules. To overcome these challenges, a lot of research needs to be carried out on the scalability and parallel connection issues of the PEM electrolyzers. In addition, effective power management and coordination control strategies are needed to ensure satisfactory and safe operation for the electrolyzers when scaled up.

5.4. *High-pressure operation*

High-pressure operation enforces the process of gas permeation through the membrane of the electrolyzer. Under elevated pressure conditions, the hydrogen gas migrates from the cathode to the anode where it will find plenty of oxygen to react and show big and dangerous explosions inside the electrolyzer compartments or gas separators. Increasing the thickness of the membrane is a key parameter here to limit and restrict the passage of hydrogen through the membrane from cathode to anode. However, increasing the thickness of the membrane will also increase the membrane ohmic resistance and thus increase the power loss of the electrolyzer and reduce its overall efficiency. Effective techniques are needed to evacuate the reaction sites from produced gases once they are generated as well as improved materials for the membrane would help reduce the effect of bubble formation, gas permeation, and water starvation at the reaction sites due the high-pressure operation.

5.5. *Fault diagnosis*

Many parameters can affect the operation of the PEM electrolyzer. Some of these parameters are the electrolyzer's voltage and current input signals, the amount of harmonics content included in these input signals, and the operating temperature and pressure of the system. Therefore, fault diagnosis strategies are required to closely monitor these parameters and take corrective actions when needed. One of the solutions for addressing these challenges is to include the electrolyzer's output measuring and monitoring signals as feedback signals in the converter's voltage and current control loops. Electrolyzer models should be adopted to allow such monitoring and control procedures.

5.6. *Modeling circuit parameters*

The values of electrical components (resistors and capacitors) used in the electrical circuit models of the electrolyzer are all based on curve-fitted parameters. These parameters are estimated by applying parameter identification methods on a set of polarization curves which are originally drawn from experiments conducted on the electrolyzer. The main problem here is that these curves and consequently these parameters are suitable only for specific devices and operating conditions. Another challenge is the accuracy of the different parameter identification methods used for estimating these parameters. This highlights the need for effective modeling and parameter estimation procedures to help construct comprehensive and generalized models for studying the performance of PEM electrolyzers.

6. Recommendations

Based on the conducted survey, some technical recommendations and future trends have been drawn for researchers to focus on and contribute. These recommendations are as follows:

- The electrical models proposed for the electrolyzer in the literature are concerned with the sole performance of the electrolyzer cell or stack, however, effective modeling of the electrolyzer performance should consider the whole system.
- Models reported in the literature are mostly cell models. Stack models are usually determined by multiplying the cell parameters by the number of cells aggregated in series. Accurate characterization of big electrolyzer stacks should be developed by implementing field experiments for large MW scale stacks.
- Electrolyzer stacks are required to be connected in parallel to one main converter or to separate converters. More research needs to be done on connecting electrolyzers in series-parallel aggregation for achieving grid-scale hydrogen production plants.
- The estimation of the model parameters requires the use of parameter identification methods. The model parameters in the studied literature are identified using a variety of methods, however, the values varied between methods. This highlights the lack of research in the critical area of electrolyzer modeling and shows that neither the feasibility of these methods for estimating the model parameters nor the range of their accuracy have been explored in a single study.
- Effective power management and coordination control strategies should be developed to help the scalability of electrolyzers at the MW system level. The efficacy of these control procedures cannot be confirmed without having

flexible and comprehensive models of the electrolyzer that allow flexible implementation of these control strategies.
- Electrical models developed in the literature do not pay any attention to the operating temperature or pressure of the electrolyzer stack, although, the effect of these parameters on the stack efficiency can be significant. So sophisticated models and controls should consider these variables to allow accurate monitoring and control of the electrolyzer stacks.

7. Conclusion

Water electrolysis is an emerging technology for generating green hydrogen from RESs. The technology has great potential on reducing the global emissions of carbon and greenhouse gases as well as mitigating the intermittency of RESs. Amongst other types of electrolyzers, the PEM electrolyzer is considered to be the best choice for generating green hydrogen from RESs. This paper is dedicated to providing an inclusive review of the electrical circuit models proposed for the PEM electrolyzer up until this point in time. For the first time, this paper analyzed and classified the electrical models in an analogous way to the physical models under the same assumptions and operating conditions. These classifications are intended to simplify model understanding and implementations based on the specific assumptions and operating conditions that may be set up by a researcher or practicing engineer. Moreover, the paper addressed some of the challenges present in electrolyzer modeling and control. Finally, the future perspectives and technical recommendations drawn from the conducted survey are briefly explained for more research and investigations.

Data availability

No data was used for the research described in this article.

Declaration of competing interest

The authors declare that they have no known competing financial interests or personal relationships that could have appeared to influence the work reported in this paper.

Acknowledgment

The authors gratefully acknowledge the financial support from Future Fuels CRC, Australia.

Appendix

Transient response of a parallel RC circuit:

In the electrical circuit models, the activation and concentration overvoltage values are represented by a parallel RC circuit. Thus, calculating the terminal voltage of a parallel RC circuit results in the estimation of the voltage values for implementation in the electrolyzer model. The following is for the estimation of (16) which represents the activation voltage as a parallel RC circuit [33,36,64].

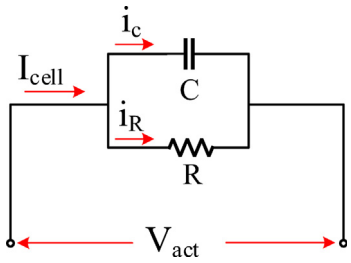

Fig. A. 1 – Parallel RC circuit diagram for estimation of activation overvoltage.

From the shown parallel RC circuit, the capacitor current can be calculated from the relation,

$$i_c = C\,\frac{d\,\eta_{act}(t)}{dt} \tag{A.1}$$

The current passing through the resistance is calculated as:

$$i_R = \frac{\eta_{act}(t)}{R} \tag{A.2}$$

Then, using Kirchhoff's current law,

$$i_{cell}(t) = i_c + i_R = C\,\frac{d\,\eta_{act}(t)}{dt} + \frac{\eta_{act}(t)}{R} \tag{A.3}$$

Taking Laplace transform, we get:

$$I_{cell}(s) = C\,[s\,V_{act}(s) - V_{act}(0)] + \frac{V_{act}(s)}{R} = \left(sC + \frac{1}{R}\right) V_{act}(s) - C\,V_{act}(0) \tag{A.4}$$

Rearranging for $V_{act}(s)$ yields:

$$\left(\frac{sRC+1}{R}\right) V_{act}(s) = I_{cell}(s) + C\,V_{act}(0) \Longrightarrow + \frac{\tau}{1+\tau s}\,V_{act}(0) \tag{A.5}$$

where $V_{act}(0)$ is the initial value of activation overvoltage at time $t = 0$, and $\tau = RC$ is the time constant of the parallel RC circuit. Applying the inverse Laplace transform we get:

$$\eta_{act}(t) = R\,.\,L^{-1}\left[\frac{1}{1+\tau s}\int_0^{\infty} i_{cell}(t)\,e^{-st}dt\right] + \eta_{act}(0)\,e^{-\frac{t}{\tau}} \tag{A.6}$$

If the current is assumed to be changed in a step form, the current equation can be written as:

$$i_{cell}(t) = \begin{cases} I_1 & t < t_c \\ I_2 & t \geq t_c \end{cases} \tag{A.7}$$

where I_1, I_2 are the current value before and after the change and t_c is the time of change expressed in seconds. Substituting (A.7) into (A.6) and applying the second theorem of translation:

$$\eta_{act}(t)=\begin{cases} R\ .\ I_1\ .\left(1-e^{-\frac{t}{\tau}}\right)+\eta_{act}(0)\ .\ e^{-\frac{t}{\tau}} & t<t_c \\ R\ .\ \left[(I_2-I_1)\left(1-e^{\frac{t_c-t}{\tau}}\right)+I_1\ .\left(1-e^{-\frac{t}{\tau}}\right)\right]+\eta_{act}(0)\ .\ e^{-\frac{t}{\tau}} & t\geq t_c \end{cases} \tag{A.8}$$

It can be reduced to:

$$\eta_{act}(t)=\begin{cases} R\ .\ f(t)+g(t) & t<t_c \\ R\ .\ \left[(I_2-I_1)\left(1-e^{\frac{t_c-t}{\tau}}\right)+f(t)\right]+g(t) & t\geq t_c \end{cases} \tag{A.9}$$

Assuming that,

$$f(t)=I_1\ .\left(1-e^{-\frac{t}{\tau}}\right) \tag{A.10}$$

$$g(t)=\eta_{act}(0)\ .\ e^{-\frac{t}{\tau}} \tag{A.11}$$

$$\tau=RC=\frac{\eta_{act}}{i_{cell}}\ .\ C \tag{A.12}$$

REFERENCES

[1] Taibi E, Miranda R, Vanhoudt W, Winkel T, Lanoix J-C, Barth F. Hydrogen from renewable power: technology outlook for the energy transition. 2018.

[2] IEA. The role of CCUS in low-carbon power systems 2020. France: International Energy Agency Paris; 2020.

[3] Kojima H, Nagasawa K, Todoroki N, Ito Y, Matsui T, Nakajima R. Influence of renewable energy power fluctuations on water electrolysis for green hydrogen production. Int J Hydrogen Energy 2023;48(12):4572–93.

[4] Eichman JD, Koleva M, Guerra Fernandez OJ, McLaughlin B. Optimizing an integrated renewable-electrolysis system. National Renewable Energy Lab. (NREL) 2020. https://doi.org/10.2172/1606147. Golden, CO (United States).

[5] Kar SK, Sinha ASK, Bansal R, Shabani B, Harichandan S. Overview of hydrogen economy in Australia. Wiley Interdisciplinary Reviews: Energy Environ 2023;12(1):e457.

[6] COAG Energy Council Hydrogen Working Group. Australia's national hydrogen strategy. 2019.

[7] Mahmoud MM, Ratib MK, Aly MM, Abdel–Rahim A-MM. Application of whale optimization technique for evaluating the performance of wind-driven PMSG under harsh operating events. Process Integration and Optimization for Sustainability 2022;6(2):447–70.

[8] Owusu P, Asumadu-Sarkodie S. "A review of renewable energy sources, sustainability issues and climate change mitigation. Cogent Eng 2016;3:1167990.

[9] Owusu PA, Asumadu-Sarkodie S. A review of renewable energy sources, sustainability issues and climate change mitigation. Cogent Engineering 2016;3(1):1167990.

[10] Mazza A, Bompard E, Chicco G. Applications of power to gas technologies in emerging electrical systems. Renew Sustain Energy Rev 2018;92:794–806.

[11] Dawood F, Anda M, Shafiullah G. Hydrogen production for energy: an overview. Int J Hydrogen Energy 2020;45(7):3847–69.

[12] Samani AE, De Kooning JD, Blanco CAU, Vandevelde L. Flexible operation strategy for formic acid synthesis providing frequency containment reserve in smart grids. Int J Electr Power Energy Syst 2022;139:107969.

[13] Dozein MG, De Corato AM, Mancarella P. Virtual inertia response and frequency control ancillary services from hydrogen electrolyzers. IEEE Trans. Power Syst. Jun 2022;38(3):2447–59.

[14] Mandal A, Muttaqi KM, Sutanto D, Islam MR. Enhanced performance of solid state transformer integrated distribution system. 2022 IEEE IAS GlobalConference on Emerging Technologies (GlobConET), 20. IEEE; 2022 May 20. p. 1056–62.

[15] Mahmoud MM, Ratib MK, Raglend J, Swaminathan J, Aly MM, Abdel-Rahim A-MM. Application of grey wolf optimization for PMSG-based WECS under different operating conditions: performance assessment. In: *2021 Innovations in Power and Advanced Computing Technologies (i-PACT)*. IEEE; 2021. p. 1–7.

[16] Madden B, Wilson M. Gigastack: bulk supply of renewable hydrogen. Cambridge: Element Energy; 2020.

[17] Gandía LM, Oroz R, Ursúa A, Sanchis P, Diéguez PM. Renewable hydrogen production: performance of an alkaline water electrolyzer working under emulated wind conditions. Energy Fuel 2007;21(3):1699–706.

[18] Chiesa N, Korpås M, Kongstein O, Ødegård A. Dynamic control of an electrolyser for voltage quality enhancement. In: Proc. of the Int. Conf. Power Systems Transients (IPST2011); Jun 2011.

[19] Zhang H, Lu Y, Zhang J, Benigni A. Real-time simulation of an electrolyzer with a diode rectifier and a three-phase interleaved buck converter. In: 2022 IEEE 13th Int. Symp. Power Electronics Dist. Gen. Syst. (PEDG). IEEE; 2022. p. 1–6.

[20] Tijani AS, Rahim AA. Numerical modeling the effect of operating variables on Faraday efficiency in PEM electrolyzer. Procedia Technology 2016;26:419–27.

[21] Ganjehsarabi H. Performance assessment of solar-powered high pressure proton exchange membrane electrolyzer: a case study for Erzincan. Int J Hydrogen Energy 2019;44(20):9701–7.

[22] Koundi M, EL Fadil H. Mathematical modeling of PEM electrolyzer and design of a voltage controller by the SMPWM approach. In: *2019 Int. Conf. Power Gen. Syst. Renewable Energy Technologies (PGSRET)*. IEEE; 2019. p. 1–6.

[23] Gusain D, Cvetković M, Bentvelsen R, Palensky P. Technical assessment of large scale PEM electrolyzers as flexibility service providers. In: 2020 IEEE 29th Int. Symp. Indust. Elect. (ISIE). IEEE; 2020. p. 1074–8.

[24] Sharifian S, Asasian Kolur N, Harasek M. Transient simulation and modeling of photovoltaic-PEM water electrolysis. Energy Sources, Part A Recovery, Util Environ Eff 2020;42(9):1097–107.

[25] Stansberry JM, Brouwer J. Experimental dynamic dispatch of a 60 kW proton exchange membrane electrolyzer in power-to-gas application. Int J Hydrogen Energy 2020;45(16):9305–16.

[26] Virji M, Randolf G, Ewan M, Rocheleau R. Analyses of hydrogen energy system as a grid management tool for the Hawaiian Isles. Int J Hydrogen Energy 2020;45(15):8052–66.

[27] Correa G, Marocco P, Muñoz P, Falagüerra T, Ferrero D, Santarelli M. Pressurized PEM water electrolysis: dynamic modelling focusing on the cathode side. Int J Hydrogen Energy 2022;47(7):4315–27.

[28] Hancke R, Holm T, Ulleberg Ø. The case for high-pressure PEM water electrolysis. Energy Conv Manag 2022;261(1):115642.
[29] Crespi E, Guandalini G, Mastropasqua L, Campanari S, Brouwer J. Experimental and theoretical evaluation of a 60 kW PEM electrolysis system for flexible dynamic operation. Energy Conv Manag 2023;277:116622.
[30] Dong Y, Ma S, Han Z, Bai J, Wang Q. Research on the adaptability of proton exchange membrane electrolysis in green hydrogen–electric coupling system under multi-operating conditions. Energy Rep 2023;9:4789–98.
[31] Hemauer J, Rehfeldt S, Klein H, Peschel A. Performance and cost modelling taking into account the uncertainties and sensitivities of current and next-generation PEM water electrolysis technology. Int. J Hydrogen Energy Aug 2023;48(66):25619–34.
[32] Koo T, Ko R, Ha D, Han J. Development of model-based PEM water electrolysis HILS (Hardware-in-the-Loop simulation) system for state evaluation and fault detection. Energies 2023;16(8):3379.
[33] Hernández-Gómez Á, Ramirez V, Guilbert D, Saldivar B. Development of an adaptive static-dynamic electrical model based on input electrical energy for PEM water electrolysis. Int J Hydrogen Energy 2020;45(38):18817–30.
[34] Samani AE, D'Amicis A, De Kooning JD, Bozalakov D, Silva P, Vandevelde L. Grid balancing with a large-scale electrolyser providing primary reserve. IET Renew Power Gener 2020;14(16):3070–8.
[35] Tuinema BW, Adabi E, Ayivor PK, García Suárez V, Liu L, Perilla A, Ahmad Z, Rueda Torres JL, van der Meijden MA, Palensky P. Modelling of large-sized electrolysers for real-time simulation and study of the possibility of frequency support by electrolysers. IET Gener Transm Distrib 2020;14(10):1985–92.
[36] Hernández-Gómez Á, Ramirez V, Guilbert D, Saldivar B. Cell voltage static-dynamic modeling of a PEM electrolyzer based on adaptive parameters: development and experimental validation. Renew Energy 2021;163:1508–22.
[37] Nguyen BL, Panwar M, Hovsapian R, Nagasawa K, Vu TV. Power converter topologies for electrolyzer applications to enable electric grid services. In: IECON 2021–47th Annual Conf. IEEE Indust. Elect. Society. IEEE; 2021. p. 1–6.
[38] Raj J, Rajasree S. A microgrid with hybrid solar-fuel cell system with CHP application. In: 2022 IEEE 2nd Int. Conf. Sust. Energy and Future Electric Transportation (SeFeT). IEEE; 2022. p. 1–6.
[39] Ram V, Salkuti SR. Modelling and simulation of a hydrogen-based hybrid energy storage system with a switching algorithm. World Electric Vehicle Journal 2022;13(10):188.
[40] Koundi M, El Fadil H, EL Idrissi Z, Lassioui A, Intidam A, Bouanou T, Nady S, Rachid A. Investigation of hydrogen production system-based PEM EL: PEM EL modeling, DC/DC power converter, and controller design approaches. Cleanroom Technol 2023;5(2):531–68.
[41] Wilberforce T, Olabi A, Imran M, Sayed ET, Abdelkareem MA. System modelling and performance assessment of green hydrogen production by integrating proton exchange membrane electrolyser with wind turbine. Int J Hydrogen Energy 2023;48(32):12089–111.
[42] Melo DFR, Chang-Chien L-R. Synergistic control between hydrogen storage system and offshore wind farm for grid operation. IEEE Trans Sustain Energy 2013;5(1):18–27.
[43] Luta DN, Raji AK. Energy management system for a remote renewable fuel cell system. In: *2019 Int. Conf. Domestic Use of Energy (DUE)*. IEEE; 2019. p. 20–4.
[44] Arsad A, Hannan M, Al-Shetwi AQ, Begum R, Hossain M, Ker PJ, et al. Hydrogen electrolyser technologies and their modelling for sustainable energy production: a comprehensive review and suggestions. Int J Hydrogen Energy 2023;48(72):27841–71.
[45] Sorrenti I, Zheng Y, Singlitico A, You S. Low-carbon and cost-efficient hydrogen optimisation through a grid-connected electrolyser: the case of GreenLab skive. Renew Sustain Energy Rev 2023;171:113033.
[46] Falcão D, Pinto A. A review on PEM electrolyzer modelling: guidelines for beginners. J Clean Prod 2020;261:121184.
[47] Järvinen L, Puranen P, Kosonen A, Ruuskanen V, Ahola J, Kauranen P, et al. Automized parametrization of PEM and alkaline water electrolyzer polarisation curves. Int J Hydrogen Energy 2022;47(75):31985–2003.
[48] Folgado FJ, González I, Calderón AJ. Simulation platform for the assessment of PEM electrolyzer models oriented to implement digital Replicas. Energy Convers Manag 2022;267:115917.
[49] Hernández-Gómez Á, Ramirez V, Guilbert D. Investigation of PEM electrolyzer modeling: electrical domain, efficiency, and specific energy consumption. Int J Hydrogen Energy 2020;45(29):14625–39.
[50] Olivier P, Bourasseau C, Bouamama PB. Low-temperature electrolysis system modelling: a review. Renew Sustain Energy Rev 2017;78:280–300.
[51] Rahim AA, Tijani AS, Kamarudin S, Hanapi S. An overview of polymer electrolyte membrane electrolyzer for hydrogen production: modeling and mass transport. J Power Sources 2016;309:56–65.
[52] Lebbal M, Lecœuche S. Identification and monitoring of a PEM electrolyser based on dynamical modelling. Int J Hydrogen Energy 2009;34(14):5992–9.
[53] Ma Z, Witteman L, Wrubel JA, Bender G. A comprehensive modeling method for proton exchange membrane electrolyzer development. Int J Hydrogen Energy 2021;46(34):17627–43.
[54] Rozain C, Millet P. Electrochemical characterization of polymer electrolyte membrane water electrolysis cells. Electrochim Acta 2014;131:160–7.
[55] Yigit T, Selamet OF. Mathematical modeling and dynamic Simulink simulation of high-pressure PEM electrolyzer system. Int J Hydrogen Energy 2016;41(32):13901–14.
[56] Toghyani S, Fakhradini S, Afshari E, Baniasadi E, Jamalabadi MYA, Shadloo MS. Optimization of operating parameters of a polymer exchange membrane electrolyzer. Int J Hydrogen Energy 2019;44(13):6403–14.
[57] Dang J, Yang F, Li Y, Zhao Y, Ouyang M, Hu S. Experiments and microsimulation of high-pressure single-cell PEM electrolyzer. Appl Energy 2022;321:119351.
[58] Ruuskanen V, Koponen J, Huoman K, Kosonen A, Niemelä M, Ahola J. PEM water electrolyzer model for a power-hardware-in-loop simulator. Int J Hydrogen Energy 2017;42(16):10775–84.
[59] Guilbert D, Vitale G. Experimental validation of an equivalent dynamic electrical model for a proton exchange membrane electrolyzer. In: *IEEE Int. Conf. Environment Electrical Eng. and 2018 IEEE Indust. and Commercial Power Syst.* Europe: EEEIC/I&CPS; 2018. p. 1–6.
[60] Guilbert D, Vitale G. Dynamic emulation of a PEM electrolyzer by time constant based exponential model. Energies 2019;12(4):750.
[61] Agbli K, Péra M, Hissel D, Rallières O, Turpin C, Doumbia I. Multiphysics simulation of a PEM electrolyser: energetic macroscopic representation approach. Int J Hydrogen Energy 2011;36(2):1382–98.
[62] Koponen J, Kosonen A, Huoman K, Ahola J, Ahonen T, Ruuskanen V. Specific energy consumption of PEM water electrolysers in atmospheric and pressurised conditions. 2016 18th European Conf. Power Elect. Applications(EPE'16 ECCE Europe). IEEE; 2016. p. 1–10.

[63] Rueda Torres J, Kumar NV, Rakhshani E, Ahmad Z, Adabi E, Palensky P, van der Meijden M. Dynamic frequency support for low inertia power systems by renewable energy hubs with fast active power regulation. Electronics 2021;10(14):1651.
[64] Hossain MB, Islam MR, Muttaqi KM, Sutanto D, Agalgaonkar AP. Dynamic electrical equivalent circuit modeling of the grid-scale proton exchange membrane electrolyzer for ancillary services. 2022 IEEE Industry Applications Society Annual Meeting (IAS). IEEE; 2022. p. 1–7.
[65] Hossain MB, Islam MR, Muttaqi KM, Sutanto D, Agalgaonkar AP. Modeling and performance analysis of renewable hydrogen energy hub connected to an ac/dc hybrid microgrid. Int J Hydrogen Energy 2022;47(66):28626–44.
[66] Khajuria R, Lamba R, Kumar R. Optimal parameter identification of PEM electrolyzer using bald eagle search optimization algorithm. In: 2022 IEEE 10th Power India Int. Conf. (PIICON). IEEE; 2022. p. 1–6.
[67] Kim J-H, Oh C-Y, Kim K-R, Lee J-P, Kim T-J. Parameter identification of electrical equivalent circuits including mass transfer parameters for the selection of the operating frequencies of pulsed PEM water electrolysis. Energies 2022;15(24):9303.
[68] Martinson CA, Van Schoor G, Uren K, Bessarabov D. Characterisation of a PEM electrolyser using the current interrupt method. Int J Hydrogen Energy 2014;39(36):20865–78.
[69] Abomazid AM, El-Taweel NA, Ez FH. Electrochemical optimization model for parameters identification of PEM electrolyzer. 2020 IEEE Electric Power and Energy Conf. (EPEC). IEEE; 2020. p. 1–5.
[70] Ali D, Gazey R, Aklil D. Developing a thermally compensated electrolyser model coupled with pressurised hydrogen storage for modelling the energy efficiency of hydrogen energy storage systems and identifying their operation performance issues. Renew Sustain Energy Rev 2016;66:27–37.
[71] Yue M, Lambert H, Pahon E, Roche R, Jemei S, Hissel D. Hydrogen energy systems: a critical review of technologies, applications, trends and challenges. Renew Sustain Energy Rev 2021;146:111180.
[72] B. Francois, D. Hissel, and M. Iqbal, "Dynamic modelling of a fuel cell and wind turbine DC-linked power system.".
[73] Dozein MG, Jalali A, Mancarella P. Fast frequency response from utility-scale hydrogen electrolyzers. IEEE Trans Sustain Energy 2021;12(3):1707–17.
[74] Marciuš D, Kovač A, Firak M. Electrochemical hydrogen compressor: recent progress and challenges. Int J Hydrogen Energy 2022;47(57):24179–93.
[75] Fragiacomo P, Genovese M. Modeling and energy demand analysis of a scalable green hydrogen production system. Int J Hydrogen Energy 2019;44(57):30237–55.
[76] van der Merwe J, Uren K, van Schoor G, Bessarabov D. A study of the loss characteristics of a single cell PEM electrolyser for pure hydrogen production. In: *2013 IEEE Int. Conf. Indust. Tech. (ICIT)*. IEEE; 2013. p. 668–72.
[77] Abomazid AM, El-Taweel NA, Farag HE. Novel analytical approach for parameters identification of PEM electrolyzer. IEEE Trans Ind Inf 2021;18(9):5870–81.
[78] Escobar-Yonoff R, Maestre-Cambronel D, Charry S, Rincón-Montenegro A, Portnoy I. Performance assessment and economic perspectives of integrated PEM fuel cell and PEM electrolyzer for electric power generation. Heliyon 2021;7(3):e06506.
[79] Khalid RM, Ahmed R. Amplitude sampled reference-based space vector pulse width modulation for control of voltage source converters. Energy Systems Research 2021;4(2):46–63.
[80] Guilbert D, Vitale G. Variable parameters model of a PEM electrolyzer based model reference adaptive system approach. In: *2020 IEEE Int. Conf. Environment Electrical Eng. and 2020 IEEE Indust. Commercial Power Syst.* Europe: IEEE; 2020. p. 1–6 (EEEIC/I&CPS Europe).
[81] Atlam O. An experimental and modelling study of a photovoltaic/proton-exchange membrane electrolyser system. Int J Hydrogen Energy 2009;34(16):6589–95.
[82] Atlam O, Kolhe M. Equivalent electrical model for a proton exchange membrane (PEM) electrolyser. Energy Convers Manag 2011;52(8–9):2952–7.
[83] Kolhe M, Atlam O. Empirical electrical modeling for a proton exchange membrane electrolyzer. In: *2011 Int. Conf. Applied Superconductivity Electromagnetic Devices*. IEEE; 2011. p. 131–4.
[84] Ayivor P, Torres J, van der Meijden M, van der Pluijm R, Stouwie B. Modelling of large size electrolyzer for electrical grid stability studies in real time digital simulation. In: Proc. 3rd Int. Hybrid Power Syst. Workshop; 2018. p. 8–9. Tenerife, Spain.
[85] Martinson C, Van Schoor G, Uren K, Bessarabov D. Equivalent electrical circuit modelling of a proton exchange membrane electrolyser based on current interruption. In: 2013 IEEE Int. Conf. Indust. Tech. (ICIT). IEEE; 2013. p. 716–21.
[86] Shen M, Bennett N, Ding Y, Scott K. A concise model for evaluating water electrolysis. Int J Hydrogen Energy 2011;36(22):14335–41.
[87] Guilbert D, Sorbera D, Vitale G. A stacked interleaved DC-DC buck converter for proton exchange membrane electrolyzer applications: design and experimental validation. Int J Hydrogen Energy 2020;45(1):64–79.
[88] Makineni RR, Sutanto D, Muttaqi KM, Islam MR, Agalgaonkar AP. Dual loop cascade control of a stacked interleaved buck converter for electrolyzer application. In: 2022 IEEE IAS Global Conf. Emerging Tech. (GlobConET). IEEE; 2022. p. 1029–35.
[89] Metwally MM, Khalid RM. Effect of grid faults on dominant wind generators for electric power system integration: a comparison and assessment. Energy Systems Research 2021;4(3):70–8.
[90] Fouda-Onana F, Chandesris M, Médeau V, Chelghoum S, Thoby D, Guillet N. Investigation on the degradation of MEAs for PEM water electrolysers part I: effects of testing conditions on MEA performances and membrane properties. Int J Hydrogen Energy 2016;41(38):16627–36.
[91] Li N, Araya SS, Kær SK. Long-term contamination effect of iron ions on cell performance degradation of proton exchange membrane water electrolyser. J Power Sources 2019;434:226755.
[92] Ratib MK, Alkhalaf S, Senjyu T, Rashwan A, Mahmoud MM, Hemeida AM, Osheba D. Applications of hybrid model predictive control with computational burden reduction for electric drives fed by 3-phase inverter. Ain Shams Eng J 2023;14(8):102028.
[93] Perry SC, de León CP, Walsh FC. The design, performance and continuing development of electrochemical reactors for clean electrosynthesis. J Electrochem Soc 2020;167(15):155525.
[94] Persson M, Mignard D, Hogg D. Insights on performance and an improved model for full scale electrolysers based on plant data for design and operation of hydrogen production. Int J Hydrogen Energy 2020;45(56):31396–409.